

3 STUDY ON DEVELOPMENT
OF TECHNIQUES FOR
RESISTANCE WELDING 2

Phases I and II 4

20 June 1966 through 6
28 February 1967 10

OR-8741

9 February 1967 1

11 Final Report
Contract No. NAS8-20339 2 III

Prepared by: D. A. Snedeker Approved by: G. O. Philip

D. A. Snedeker
Task Leader
Advanced Manufacturing
Technology Department

G. O. Philip
Manager
Advanced Manufacturing
Technology Department

Prepared for
George C. Marshall Space Flight Center
Huntsville, Alabama

1 Martin Marietta Corporation
Orlando, Florida

STUDY ON DEVELOPMENT OF TECHNIQUES
FOR RESISTANCE WELDING

by

W. R. Hutchinson
W. E. Weber
F. C. Deal
D. A. Snedeker

FOREWORD

This report was prepared by the Orlando division of Martin Marietta Corporation, Orlando, Florida under National Aeronautics and Space Administration Contract No. NAS 8-20339. The development was administered by the Manufacturing Research and Technology Division of the George C. Marshall Space Flight Center, Huntsville, Alabama.

The Martin Marietta Corporation wishes to express appreciation for the support, guidance, and cooperation from NASA technical representatives Messrs. Truitt Vann and J. D. Bennight.

In addition to the authors, a program of this type requires the services of many persons who were not directly involved in authoring the report. These persons have contributed materially to the success of this program and without whose services, the desired results would not have been achieved. Appreciation is expressed to the following persons for their parts in the program:

G. D. Yates, for his overall technical direction and helpful suggestions for enhancing the scope of the program.

R. R. Braswell, as an accomplished microelectronic welder who has successfully completed the NASA course on Reliable Electrical Connections (module welding), he performed the welds and tests necessary to complete this program. He was also instrumental in fabrication of the electronic circuitry used in the program.

R. G. Howard, for his outstanding aid in the selection of infrared sensors and in the design of optical systems.

D. W. Pease, for his invaluable aid in preparation of the metalographic samples and photomicrographs contained in this report.

CONTENTS

Summary	xiii
Introduction.	xv
I. Infrared Concept Feasibility.	1
A. Background Information.	2
B. Equipment.	2
C. Results.	8
II. Go, No-Go Visual Indicator	31
A. System Requirements	31
B. Circuit Description.	37
C. External Noise.	44
D. Future Circuit Improvements.	44
III. Pseudoweld Feasibility	45
Recommendations.	53
References	55

ILLUSTRATIONS

1	Infrared Detector	4
2	Mounted Detector Focused on the Weld Joint	4
3	Detector and Recording Equipment	4
4	Hughes VTW-30C Power Supply and Hughes VTA-60 Welding Head	5
5	Pulse Shapes from Hughes Power Supply with Specially Designed Output Transformer.	5
6	Tapped Inductor	6
7	Inductance Steps.	6
8	Pulses Shapes Resulting from Inductor.	7
9	Weld Pulse Rise Times (Slopes 1, 6, and 12).	7
10	Final Modified Output Circuit.	8
11	Infrared Radiation/Tensile Strength Correlation, 0.020 Inch Gold Plated Dumet Wire to 0.010 by 0.020 Inch Bare Nickel Ribbon, 10 Pounds Pressure	9
12	Infrared Radiation/Tensile Strength Correlation, 0.017 Inch Gold Plated Kovar Wire to 0.010 by 0.020 Inch Bare Nickel Ribbon, 8 Pounds Pressure	9
13	Infrared Radiation/Tensile Strength Correlation, 0.020 Inch Gold Plated Nickel Wire to 0.010 by 0.020 Inch Bare Nickel Ribbon, 6 Pounds Pressure	10
14	Isostrength Diagram, 0.020 Inch Gold Plated Nickel Wire to 0.010 by 0.020 Inch Bare Nickel Ribbon, Slope 1	15
15	Isostrength Diagram, 0.020 Inch Gold Plated Nickel Wire to 0.010 by 0.020 Inch Bare Nickel Ribbon, Slope 6	16
16	Isostrength Diagram, 0.020 Inch Gold Plated Nickel Wire to 0.010 by 0.020 Inch Bare Nickel Ribbon, Slope 12	17

17	Weld Pulse Rise Time, Slopes 12, 6, and 1 (Left to Right)	18
18	Weld Expulsion	18
19	Isostrength Diagram, 0.020 Inch Gold Plated Dumet Wire to 0.010 by 0.020 Inch Bare Nickel Ribbon, Slope 1	19
20	Isostrength Diagram, 0.020 Inch Gold Plated Dumet Wire to 0.010 by 0.020 Inch Bare Nickel Ribbon, Slope 6	20
21	Isostrength Diagram, 0.020 Inch Gold Plated Dumet Wire to 0.010 by 0.020 Inch Bare Nickel Ribbon, Slope 12	21
22	Isostrength Diagram, 0.017 Inch Gold Plated Kovar Wire to 0.010 by 0.020 Inch Bare Nickel Ribbon, Slope 1	22
23	Isostrength Diagram, 0.017 Inch Gold Plated Kovar Wire to 0.010 by 0.020 Inch Bare Nickel Ribbon, Slope 6	23
24	Isostrength Diagram, 0.017 Inch Gold Plated Kovar Wire to 0.010 by 0.020 Inch Bare Nickel Ribbon, Slope 12	24
25	Metallography Laboratory	25
26	0.020 Inch Dumet Wire Welded to 0.010 by 0.020 Inch Bare Nickel Ribbon	26
27	0.020 Inch Nickel Wire Welded to 0.010 by 0.020 Inch Bare Nickel Ribbon	27
28	0.017 Inch Kovar Wire Welded to 0.010 by 0.020 Inch Bare Nickel Ribbon	28
29	Kovar Wire Weld, Lead Ribbon Orientation Reversed	29
30	GO, NO-GO Visual Indicator	32
31	GO, NO-GO Test Equipment	32
32	GO, NO-GO Visual Indicator Schematic	33
33	Three Infrared Radiation Curves Resulting from Three Separate Weld Pulses, Kovar Wire	34
34	LO, NO-GO/GO Transition	35
35	GO/HI, NO-GO Transition	36
36	GO, NO-GO Visual Indicator Block Diagram	37
37	Infrared Detector and Associated Network	38
38	Impedance Matching	39
39	HI, NO-GO/GO Signal Level Detector	40

40	LO, NO-GO Signal Level Detector	41
41	HI, NO-GO Memory and Reset	42
42	GO Memory and Reset.	43
43	LO, NO-GO Memory and Reset	43
44	Pseudoweld Equipment	45
45	Effect of Pseudoweld on Weld Quality, Nickel Wire	48
46	Effect of Pseudoweld on Weld Quality, Kovar Wire	49

TABLES

I.	Infrared and Weldability Data for 0.020 Inch Diameter Dumet Lead to 0.010 by 0.020 Inch Diameter Nickel Ribbon Welds . . .	11
II.	Infrared and Weldability Data for 0.017 Inch Diameter Kovar Lead to 0.010 by 0.020 Inch Diameter Nickel Ribbon Welds . . .	12
III.	Infrared and Weldability Data for 0.020 Inch Diameter Nickel Lead to 0.010 by 0.020 Inch Diameter Nickel Ribbon Welds . . .	13
IV.	Changes in Weldability Range as a Function of Weld Pulse Shape	14
V.	Optimum Parameters Based on Isostrength Data	18
VI.	Statistical Analysis of Infrared Data from Pseudoweld Program	47
VII.	Detection of Undesirable Welds	51

PRECEDING PAGE BLANK NOT FILMED.

SUMMARY

INFRARED CONCEPT FEASIBILITY

The Infrared Concept has been conclusively verified by the results of this contract. The Infrared Concept is defined as the "correlation between infrared heat radiation and the quality of the weld joint." This important correlation provides the basis for a reliable in-process nondestructive inspection technique which is instantaneous and automatic. More than 7,000 welds, including four wire combinations most commonly used in the electronic industry, provide ample evidence that this infrared radiation technique suggests an answer to the question of consistent high quality welds under mass production requirements.

The present industry practice is to interconnect different wire materials with Nickel ribbon wire for effective resistance welding. Four wire materials, Nickel, Kovar, Dumet, and Copper, are commonly used in the electronic industry as component leads.

Statistical experiments were designed to vary the welding parameters, including watt-second energy, weld pulse rise time, and electrode pressure, for each of the wire combinations above. Simultaneous recordings were made of voltage, current, and infrared radiation. Weld strength and set-down were also recorded. This information was then statistically analyzed and correlated with visual characteristics such as expulsion, discoloration, and weld rise time variations. The resulting data confirmed the Infrared Concept by correlating closely with optimum welding parameters as derived from conventional isostrength diagrams.

GO NO-GO VISUAL INDICATOR

A GO NO-GO Visual Indicator was designed and breadboarded to implement the Infrared Concept. The Infrared Concept, as previously defined, is "the correlation between infrared heat radiation and the quality of the weld joint." Therefore, the function of the NO, NO-GO Visual Indicator is to 1) sense the IR generated at the weld joint, 2) analyze the level of IR radiated, and 3) provide a GO or NO-GO indication, by energizing one of three lamps. The lamps are referred to as LO, NO-GO, GO, and HI, NO-GO, which are red, green, and red respectively.

The GO, NO-GO Visual Indicator is adjustable for any given wire combination as determined from an IR/Tensile Correlation graph for the desired wire combination.

PSEUDOWELD FEASIBILITY

The pseudoweld concept is a Martin technique that is used as an in-process nondestructive preweld inspection. A pseudoweld is defined as "a weld made at any energy-level below the fusion threshold as long as the level is high enough to produce a detectable IR measurement."

The second phase of this program deals with the use of the pseudoweld (or low energy weld) as a technique for predicting the relative quality of a full energy weld. For this purpose, the IR energy output is measured while a weld energy level insufficient to cause bonding is applied to the various lead-ribbon material combinations. Without disturbing the lead-ribbon material position, the power level is then increased and a full strength weld performed.

The pseudoweld concept has demonstrated the ability to detect major weld conditions which contribute to, or produce, defective welds as well as a potential beneficial effect of "purging by fire." By the use of the preweld pulse or pseudoweld, the weld joint is briefly heated to temperatures just below fusion temperatures, driving off volatile contaminants before the normal full strength weld is made. This combined with the fact that the pseudoweld does not affect the strength of the normal full strength weld affords significant strides in the development of weld technology.

Preweld quality inspection may be achieved and in the future incorporated into an advance welding power supply for the fabrication of highly reliable missile components.

INTRODUCTION

Resistance welding has been rated lowest in connection reliability when compared to soldering and wirewrap connections for the geometry of certain tests. The rating resulted from a study conducted by a national laboratory skilled in the use of resistance welding. The evaluation was based on results from environmental tests (Reference 1). Since in theory welding should be one of the most reliable joining techniques, the decision given by the rating agency points out the lack of progress understanding, weldability knowledge, and equipment-material relationships. Much of the understanding of the microresistance welding technique has come from the results of such physical testing as tensile and shear tests and in the analysis of photomicrographs, all of which are destructive and performed after the fact. These tests really study the effect and not the cause.

The Orlando division of Martin Marietta Corporation used certain conventional tests in their proper perspective along with the infrared and pseudoweld tests which only recently have become available for use in programs such as this. These test techniques were developed by the Orlando division under a company-sponsored program of noncontacting test techniques (Reference 2).

Preliminary results of further work along this line has indicated that the use of infrared radiation techniques is feasible for the in-process testing of welds (to predict the pull strength of welds).

Although much knowledge and understanding of the physics of welding was gained from this study, a considerable amount of work remains to be completed before the resistance welding process is fully understood. Even more work is necessary before complete process control can be a reality.

By experimenting and analyzing the signals, responses, and circuits necessary in the development of the required hardware, the objectives are to provide the answers to such questions as what happens during the welding process, what constitutes a good weld, what parameters are the most important and which can be controlled, and how to measure and control the parameters involved.

I. INFRARED CONCEPT FEASIBILITY

The infrared concept is defined as "the correlation between infrared heat radiation and the quality of the weld joint." This important correlation provides the basis for a reliable in-process, nondestructive inspection technique which is instantaneous and automatic.

This phase of the program was directed toward establishing the relationships between the infrared radiation (IR) emitted during the weld pulse cycle with the relative tensile strength of the weld. This relationship was modified by introducing other variables such as various weld pulse rise times and welder pressure settings. The present industry practice is to interconnect wire lead materials with Nickel ribbon wire for effective resistance welding. Four of the most common wire lead materials encountered are Nickel, Kovar, Dumet, and Copper. Therefore, the wire combinations used for the experiments performed in this contract were:

- 1 Nickel ribbon (0.010 by 0.020) to Nickel wire (0.020)
- 2 Nickel ribbon (0.010 by 0.020) to Kovar wire (0.017)
- 3 Nickel ribbon (0.010 by 0.020) to Dumet wire (0.020)
- 4 Nickel ribbon (0.010 by 0.020) to Copper OHFC wire (0.020).

Individual IR measurements and weld tensile strength were recorded for each of five weld samples at specified welder energy-pressure levels. In addition peak weld voltage and current were recorded for each weld over a range from a point where the welder energy was insufficient to produce a weld, to expulsion or any visible evidence of weld spatter. Set down was measured at the 2 and 10 pound pressure settings only. The welder energy setting intervals as determined by the results of previous investigation are:

- 1 Nickel lead wire - 2 watt second
- 2 Kovar lead wire - 1/2 watt second
- 3 Dumet lead wire - 1 watt second
- 4 Copper lead wire - 1 watt second.

All lead materials noted above were gold plated. These lead materials were welded to bare 0.010 by 0.020 Nickel ribbon.

A. BACKGROUND INFORMATION

To produce a weld joint of good quality, sufficient heat must be generated at the proper location within a prescribed time span. It has been found that measuring the heat generated at the weld joint is the most reliable method of determining the quality of a weld. It is known that every object whose temperature is above absolute zero (-273°C) radiates infrared energy whose magnitude is proportional to the fourth power of the absolute temperature of the radiating surface. Stefan - Boltzmann's law (Reference 3) states that

$$W = E\sigma T^4$$

where

W = total radiant flux per unit area

E = surface emissivity constant*

σ = Stefan - Boltzmann's constant

T = surface temperature ($^{\circ}\text{K}$).

Thus, the measurement of IR is ideally suited for determining heat generation at the weld joint and therefore, the weld quality. Infrared detection components have been significantly advanced to permit infrared measurements from small targets such as a microweld.

B. EQUIPMENT

1. Infrared Detectors

Since an IR detector suitable for the specialized function in these experiments was not available at the start of the contract, a detector was built considering the most important factors of: 1) Sensitivity in the temperature range to be detected; 2) working distance, and 3) ease of detector alignment.

*Since relative and not absolute power is to be measured, no problems with emissivity are anticipated.

The temperature of the weld joint is determined by the fusion point of the materials to be welded. Gold has the lowest fusion point at 1060°C, and iron has the highest fusion point at 1535°C. The temperature to be detected was therefore assumed to range between 1000°C and 1600°C for all material combinations. This temperature range produces a blackbody radiation curve which peaks at approximately 3.5 microns (μ).

Two sensor materials were selected: Indium arsenide, a photovoltaic type, and lead sulfide, a photoconductive type, both having response peaks close to the radiation peak. The spectral response and sensitivity of both types of sensors were found to be comparable, with the lead sulfide type slightly more sensitive. Since indium arsenide was reported to have a long term drop in sensitivity, it was rejected in favor of lead sulfide.

The selected sensor's active area measures 1 by 1 millimeter (mm) in order to minimize variations in the sensitivity across the sensor element. Working distance between the sensor housing and the weld tips was limited to approximately 3/8 inch. This was required to allow the welder operator sufficient clearance to properly align, clean, and adjust the weld electrodes.

Two optical systems were designed and constructed to focus the weld energy on the sensor element. A reflecting system (1 1/4 inches diameter by 5/8 inch long) was evaluated and found to have a working distance of 1 inch from the weld joint. However, this unit was very difficult to align both internally and with the workpiece. The refracting system was evaluated and it was found that the working distance could be reduced to 1/2 inch because of its reduced diameter. This decrease in distance overcame the slightly lower optical speed of this system as compared to the reflecting system and also the slight transmission loss through the lens.

The final system (Figure 1) was constructed utilizing thin wall brass tubing with inserts holding the internal components in place. This type construction eliminated internal alignment problems and simplified construction. The unit housing is 2 1/4 inches long by 3/8 inch diameter. The optical system has a field of view of 1/8 inch at a working distance of 1/2 inch and a speed of f:1.5. Figure 2 shows the detector in the mounted position focused on the weld joint. The detector and recording equipment are shown in Figure 3.

2. Power Supply

Initial tests of the weld power supply verified the assumption that the rise time of the slope was independent of the power output. The inherent rise time of the weld power supply was determined to be approximately 0.76 milliseconds.

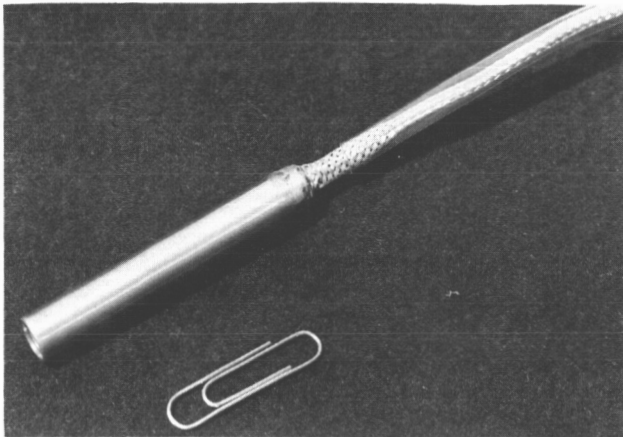


Figure 1. Infrared Detector

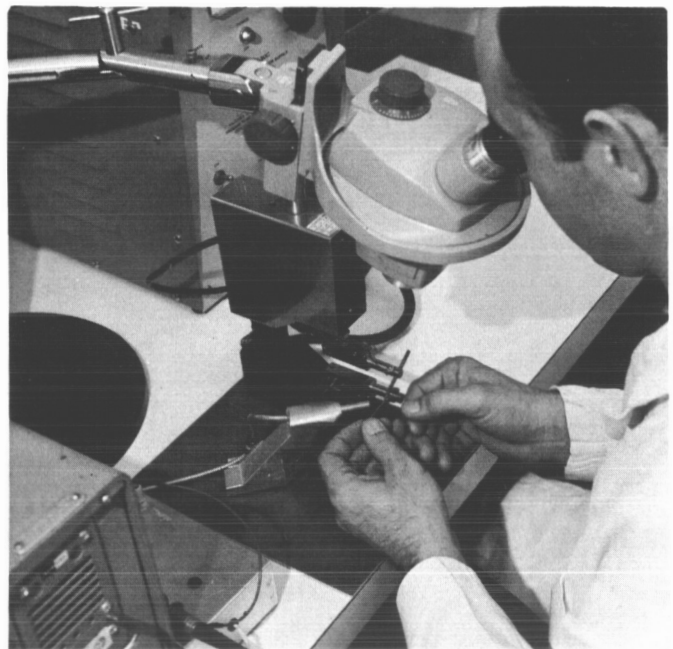


Figure 2. Mounted Detector
Focused on The Weld Joint



Figure 3. Detector and
Recording Equipment

A specially designed three tap output transformer was purchased from Hughes and installed in the Hughes Model VTW-30C Power Supply (Figure 4). The resultant pulse shapes (Figure 5) were evaluated and considered not to be spaced far enough apart for this study.

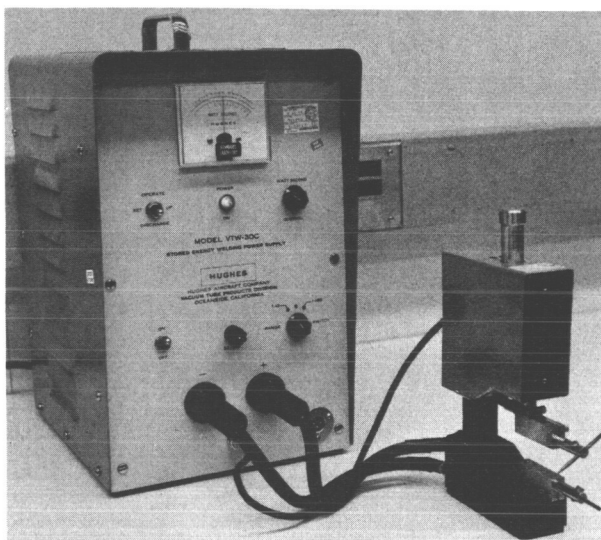
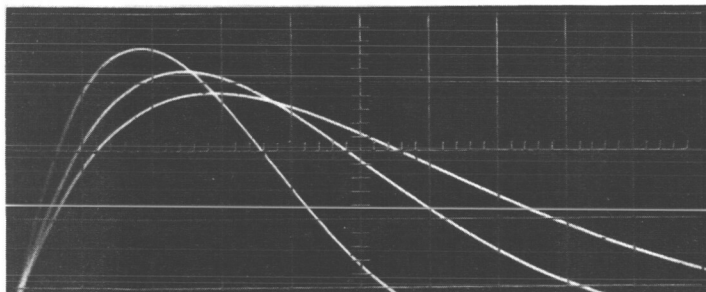


Figure 4. Hughes VTS-30C Power Supply and Hughes VTA-60 Welding Head



Horizontal: 1 ms/cm
Vertical: 5 mV/cm

Figure 5. Pulse Shapes from Hughes Power Supply with Specially Designed Output Transformer

To obtain a minimum of three different pulse shapes, the power supply (which was designed to produce only one pulse shape) was modified to produce a selection of ten additional pulse shapes. The modification was by a tapped inductor (Figures 6 and 7) which was designed for insertion in the

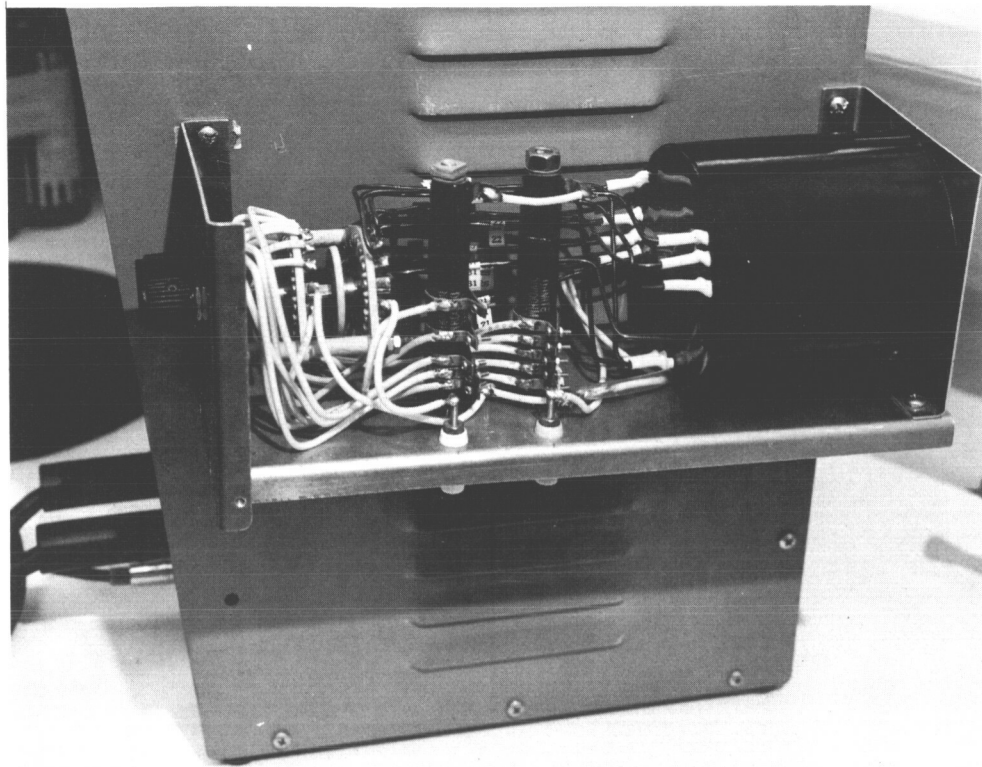
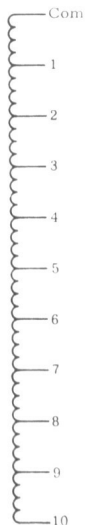


Figure 6. Tapped Inductor

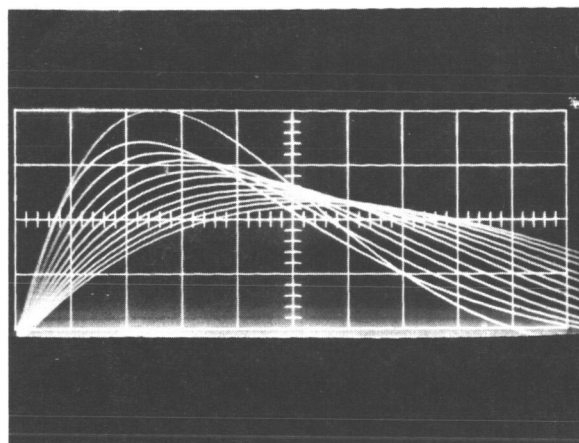
primary circuit of the output transformer to produce a wider variation of pulse shapes. The inductor changed the pulse shape by increasing the weld pulse rise time, therefore increasing the time required to reach a content sufficient to cause a welded bond. The inductor provided ten different pulse shapes which ranged from 0.76 to 2.25 milliseconds rise time in ten steps (Figure 8) as measured across a 500A shunt.



Tap	Ind (μ h)	Res (Ω)
1	200	0.23
2	400	0.39
3	600	0.48
4	800	0.57
5	1,000	0.66
6	1,200	0.75
7	1,400	0.81
8	1,600	0.89
9	1,800	0.97
10	2,000	1.10

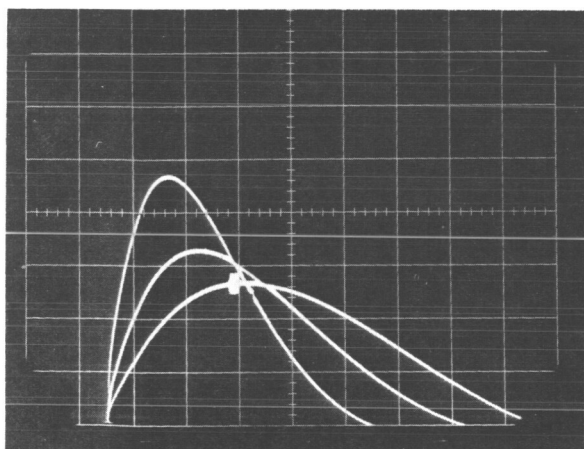
Figure 7. Inductance Steps

Figure 8. Pulses Shapes Resulting from Inductor



Horizontal: 0.5 ms/cm
Vertical: 50 mV/cm

Three of the weld pulse rise times (Slopes 1, 6, and 12) were chosen for the statistical experiments (Figure 9). The highest amplitude curve is the original unmodified pulse shape, which was left intact and is referred to as Slope 1. Each lower amplitude curve is the result of additional inductance. Slope 6 is a setting which has 40 percent of the maximum inductance in the circuit. Slope 12 represents the maximum inductance value.



Horizontal: 1 ms/cm
Vertical: 0.05 V/cm

Figure 9. Weld Pulse Rise Times
(Slopes 1, 6, and 12)

Compensation was added to the circuit to maintain a constant energy output as the inductance changed from 0 to 2000 microhenrys through the ten steps. The final modified output circuit is shown in Figure 10.

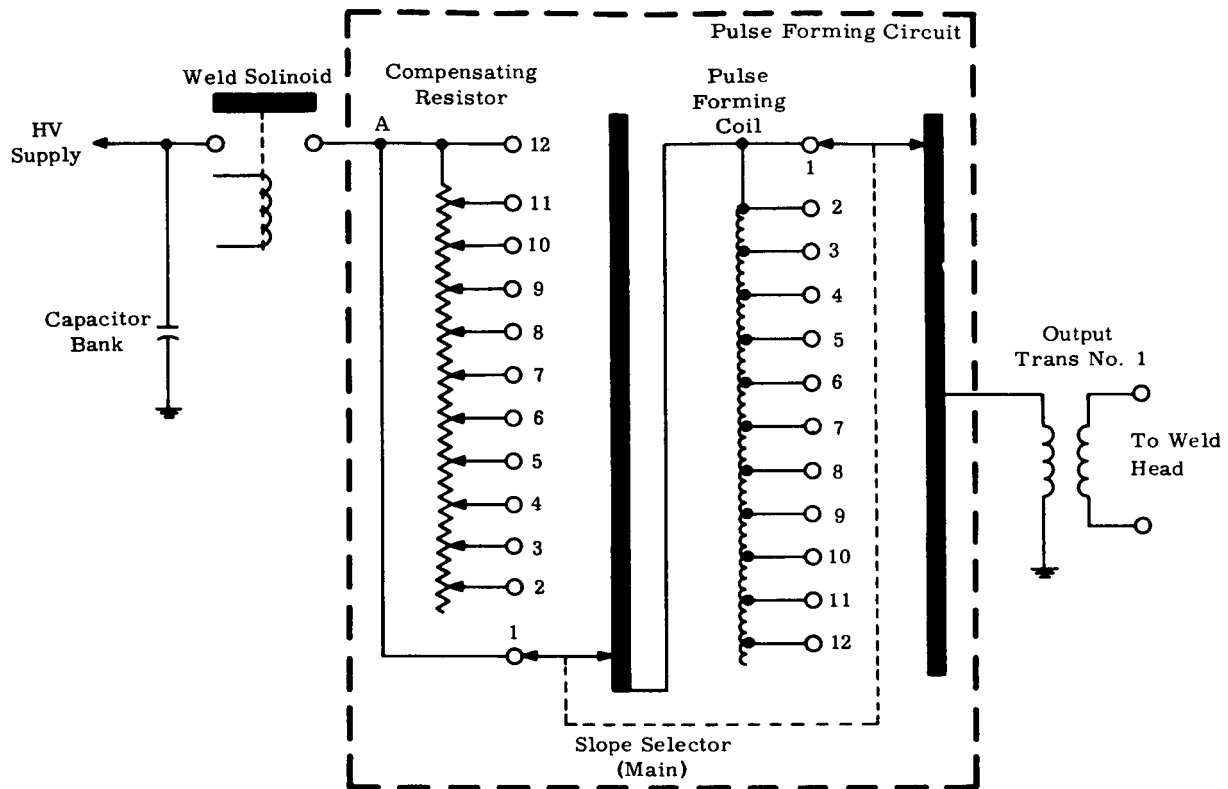


Figure 10. Final Modified Output Circuit

C. RESULTS

1. Infrared Concept

An evaluation of the IR - weld tensile strength data has shown a definite correlation. Typical graphs plotting tensile strength and IR emission versus the welder input energy are shown in Figures 11, 12, and 13. The graphs shown are for the lead materials of 0.020 diameter Dumet, 0.017 diameter Kovar and 0.020 diameter nickel wire welded to a 0.010 by 0.020 Nickel 205 ribbon. Only gold plated lead materials welded to bare ribbon are presented since this appeared to be the most desirable surface condition combination. These graphs also show the effect of increasing the weld pulse rise time (i.e., increasing the time required to reach a heat content that is sufficient for a weld) on the useful weldability range. This range is calculated by determining the watt-second energy range between the weld strength value which represents 60 percent of the tensile strength of the weaker member of the joint, and the point just before expulsion or violation of the set-down requirements. This weldability range is expressed in watt-seconds.

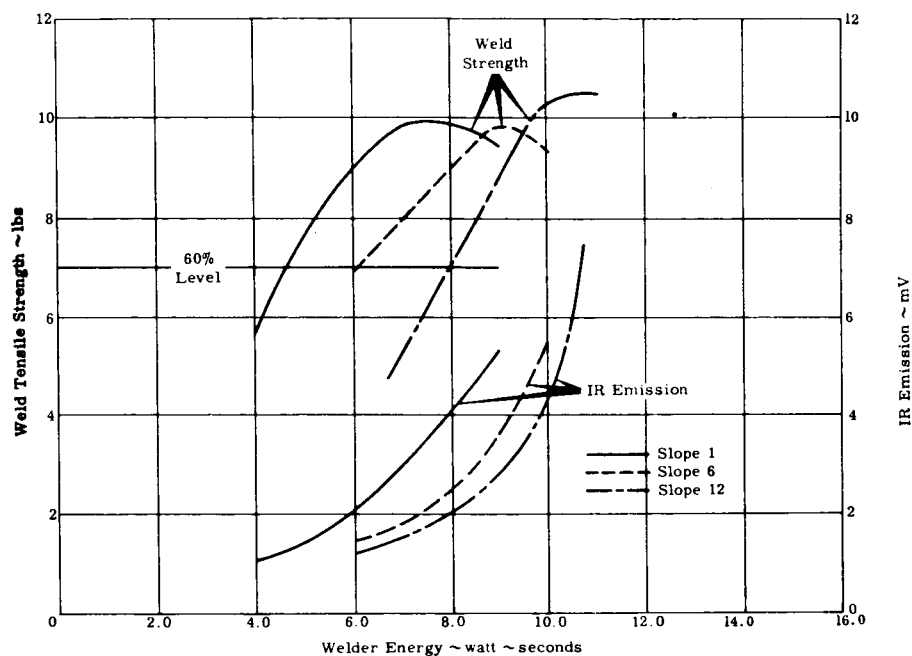


Figure 11. Infrared Radiation/Tensile Strength Correlation, 0.020 Inch Gold Plated Dumet Wire to 0.010 by 0.020 Inch Bare Nickel Ribbon, 10 Pounds Pressure

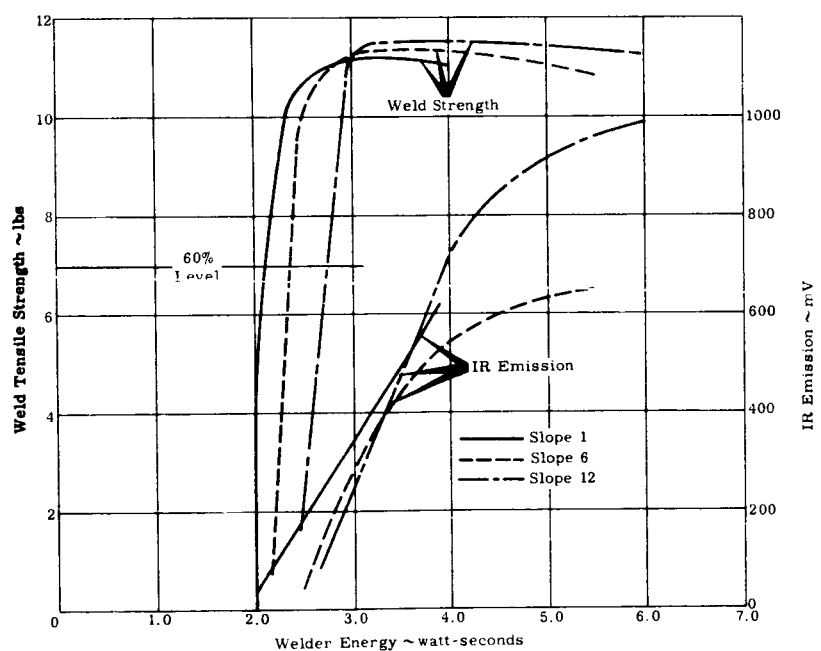


Figure 12. Infrared Radiation/Tensile Strength Correlation, 0.017 Inch Gold Plated Kovar Wire to 0.010 by 0.020 Inch Bare Nickel Ribbon, 8 Pounds Pressure

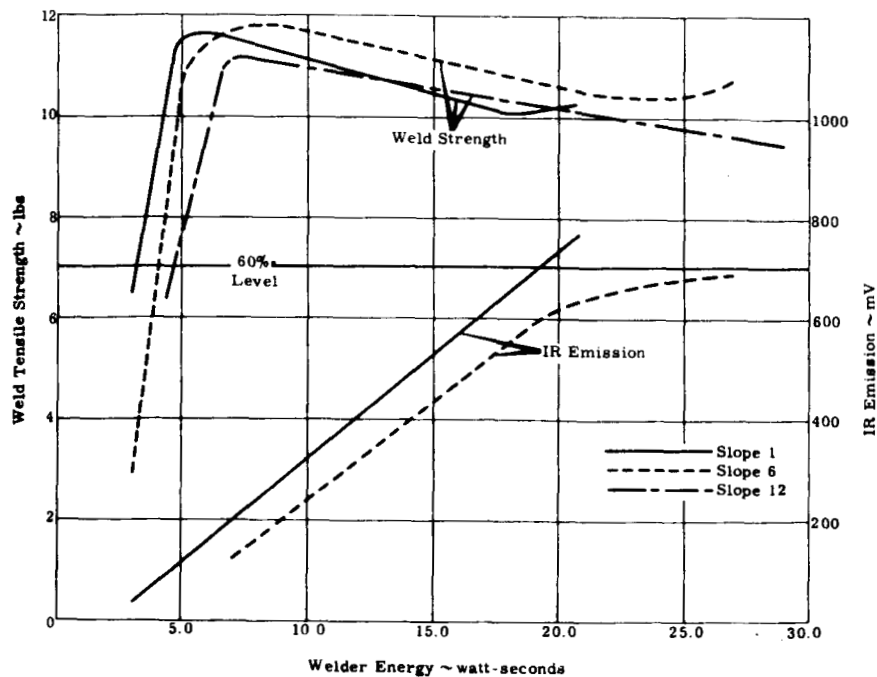


Figure 13. Infrared Radiation/Tensile Strength Correlation, 0.020 Inch Gold Plated Nickel Wire to 0.010 by 0.020 Inch Bare Nickel Ribbon, 6 Pounds Pressure

The IR curves approach linearity as a function of increasing welder input energy. From these curves it is possible to extrapolate lines from the point describing the minimum of the weldability range to the IR curve. Likewise the point on the tensile strength curve representing the maximum of the weldability range, if read on the IR curve, will determine the upper limit of IR emission. Combining these two values will describe the bounds of IR emission for acceptable welds. These values are shown in Tables I, II, III. Included in these tables is a comparison of the effect of changing the weld pulse shape on the weldability range.

In the conceptual stages of the IR detection technique, it was thought desirable that the IR limits be maintained as restrictive as possible so as to make use of the in-process inspection potential of the system. In addition, it was postulated that if the weld pulse shape could be controlled by attenuating the amplitude of the heat curve, a wider weldability range would result. These tables are especially informative in this respect and will be analyzed individually.

1) Dumet Lead (Table I)

The usable IR range for Slopes 1 and 6 continue to be reduced as the welder pressure is raised; however, the data for Slope 12 appears to be erratic and does not follow the same pattern. The weldability range does not show a significant improvement until the 14 pound pressure level is reached, where a marked change is noted. Examination of the 14 pound pressure level shows the lowest overall IR spread with improved weldability range when a limited inductance (Slope 6) is introduced for weld pulse shape control. A significant improvement was achieved at this pressure level. All welds were well above minimum strength requirements and within deformation limitations. This degree of improvement is not apparent at the other pressure levels.

TABLE I

Infrared and Weldability Data for 0.020 Inch Diameter
Dumet Lead to 0.010 by 0.020 Inch Diameter
Nickel Ribbon Welds

Welder Pressure Level (lb)		Slope 1		Slope 6		Slope 12	
		IR (mV)	Weld (WS)	IR (mV)	Weld (WS)	IR (mV)	Weld (WS)
2	Data spread	125-375	3.8-7.0	140-325	5.4-9.0	130-170	5.5-6.0
	Range	250	3.2	185	3.6	40	0.5
4	Data spread	125-285	4.4-7.0	125-280	6.2-9.0	125-230	5.8-8.0
	Range	160	2.6	155	2.8	105	
6	Data spread	110-245	4.4-8.0	105-255	5.7-9.0	135-250	7.2-8.0
	Range	135	3.6	150	3.3	115	0.8
8	Data spread	100-285	4.7-9.0	100-220	6.4-9.0	125-175	7.3-8.0
	Range	185	4.3	120	2.6	50	0.7
10	Data spread	65-185	4.7-8.0	80-195	6.2-9.0	145-270	9.1-10.0
	Range	120	3.3	115	2.8	125	0.9
12	Data spread	60-165	5.0-8.0	60-160	6.7-10.0	65-105	7.5-9.0
	Range	105	3.0	100	3.3	40	1.5
14	Data spread	40-100	5.4-9.0	35-100	10-17	45-70	8.3-13.0
	Range	60	3.6	65	7.0	25	4.7

2) Kovar Lead (Table II)

The weldability of this material appears to respond to only a limited degree with the addition of weld pulse shape control. In the unmodified equipment, an optimum IR range is achieved at 6 pounds pressure whereas the Slope 6 setting shows the most restrictive range to be at 12 pounds. Because of the extreme limits, the Slope 12 results did not indicate an advantage. The data show an improvement in the weldability range at all but one pressure level for Slope 6 when compared with that of Slope 1. Continued improvement is noted in the Slope 12 weldability results only at the higher pressure levels. Since the narrow IR band is the dominant requirement, the improvements noted in the Slope 12 weldability results are nullified.

TABLE II

Infrared and Weldability Data for 0.017 Inch Diameter
Kovar Lead to 0.010 by 0.020 Inch Diameter
Nickel Ribbon Welds

Welder Pressure Level (lb)		Slope 1		Slope 6		Slope 12	
		IR (mV)	Weld (WS)	IR (mV)	Weld (WS)	IR (mV)	Weld (WS)
2	Data spread	80-880	1.7-5.0	80-940	2.1-6.0	150-830	2.25-5.0
	Range	800	3.3	860	3.9	680	2.75
4	Data spread	100-600	1.75-4.0	85-760	2.15-5.0	70-820	2.35-5.0
	Range	500	2.25	675	2.85	750	2.65
6	Data spread	90-475	1.8-3.5	120-560	2.3-4.0	130-760	2.65-4.0
	Range	385	1.7	440	1.7	630	1.35
8	Data spread	110-570	2.2-3.5	110-610	2.7-5.0	220-960	2.8-5.5
	Range	460	1.3	500	2.3	740	2.7
10	Data spread	130-620	2.3-5.0	220-620	3.25-7.0	180-980	3.2-7.5
	Range	490	2.7	400	3.75	800	4.3
12	Data spread	130-625	2.3-5.0	250-620	3.3-7.0	-	3.2-10.0
	Range	495	2.7	370	3.7	-	6.8

3) Nickel Lead (Table III)

The modifications made in the amplification equipment resulted in a scale factor change. As a result, the IR range data for Slope 12 and the 14 pound pressure level cannot be correlated with previous data and, therefore, are not presented in this table. A review of the limited data in Table III shows a general trend to improved weldability range at all slopes as the pressure level is increased. It will be noted that the IR range is similarly increased. Although this increase would appear to be detrimental when comparing the results with the Kovar and Dumet lead materials, it must be remembered that the IR output continues to rise as the welder energy

TABLE III
Infrared and Weldability Data for 0.020 Inch Diameter
Nickel Lead to 0.010 by 0.020 Inch Diameter
Nickel Ribbon Welds

Welder Pressure Level (lb)		Slope 1		Slope 6		Slope 12	
		IR (mV)	Weld (WS)	IR (mV)	Weld (WS)	IR (mV)	Weld (WS)
2	Data spread	70-325	2.8-7.0	40-450	3.6-11.0	*	3.75-15
	Range	225	4.2	410	7.4	-	11.25
4	Data spread	45-310	2.8-9.0	45-625	3.9-17.0	-	4.2-19.0
	Range	265	6.2	580	13.1	-	14.8
6	Data spread	40-710	3.2-19.0	50-690	4.5-25.0	-	4.6-27.0
	Range	670	15.8	640	20.5	-	22.4
8	Data spread	60-690	3.5-27.0	20-650	4.5-29.0	-	5.0-31.0
	Range	630	23.5	630	24.5	-	25.0
10	Data spread	20-770	5.5-35.0	15-730	5.5-39.0	-	6.5-41.0
	Range	750	29.5	715	33.5	-	34.5
12	Data spread	20-690	4.8-37.0	25-550	6.4-43.0	-	6.6-45.0
	Range	670	32.2	525	36.6	-	38.4
14	Data spread	-	7.6-37.0	-	8.0-57.0	-	8.1-51.0
	Range	-	29.4	-	49.0	-	42.9

*Not reported, improved IR amplification system not correlatable with other data.

input is increased. Since the weldability range was much greater for Nickel than for any other material combination, a much greater portion of the total IR emission curve is being used. It can be seen that the IR range is proportional to the increased weldability range. The effect of adding of weld pulse shape control on the weldability range can be seen in Table IV. The percent increases are shown in comparison with the unmodified welder.

TABLE IV

Changes in Weldability Range as a Function of Weld Pulse Shape

Pressure (lb)	Slope 6	Slope 12
2	+43.3%	+62.5%
4	+52.7	+56.7
6	+22.9	+29.4
8	+ 4.1	+ 6.0
10	+11.9	+14.5
12	+12.0	+16.1
14	+40.0%	+31.5%

The most significant improvement in the weldability range is achieved at the extremes of the pressure limits. A small change in the weld pulse rise time (Slope 6) results in marked improvement in the weldability range. Additional manipulation of the weld pulse does not result in a proportional increase.

As an example, the tensile strength data for gold plated nickel lead material is shown as a function of welder energy input and welder pressure on Figures 14 through 16. These isostrength diagrams show the effect of increasing the weld pulse rise time on the weldability range. The values under the individual points indicate average and range of tensile strength. The actual shape of these weld pulses can be seen in Figure 17. The order from right to left is Slope 1, Slope 6 and Slope 12. Although the amplitude of the heat content curve is reduced as the weld pulse rise time increases, the total heat input remains the same. The increase in the weldability range with increasing weld pulse rise time, as shown in Table IV must be the result of attenuating the amplitude of the heat curve. It is theorized that as higher energy welds are made, the vaporization temperature of the joint material combination is being constantly approached. The use of weld pulse rise time control prevents the uncontrollable surges that would cause expulsion. Therefore the maximum energy level can be more closely approached without the danger of causing premature expulsion. As compared to Figure 17 which shows the shape of the IR curve for an acceptable weld, Figure 18 is a representative trace exhibiting expulsion.

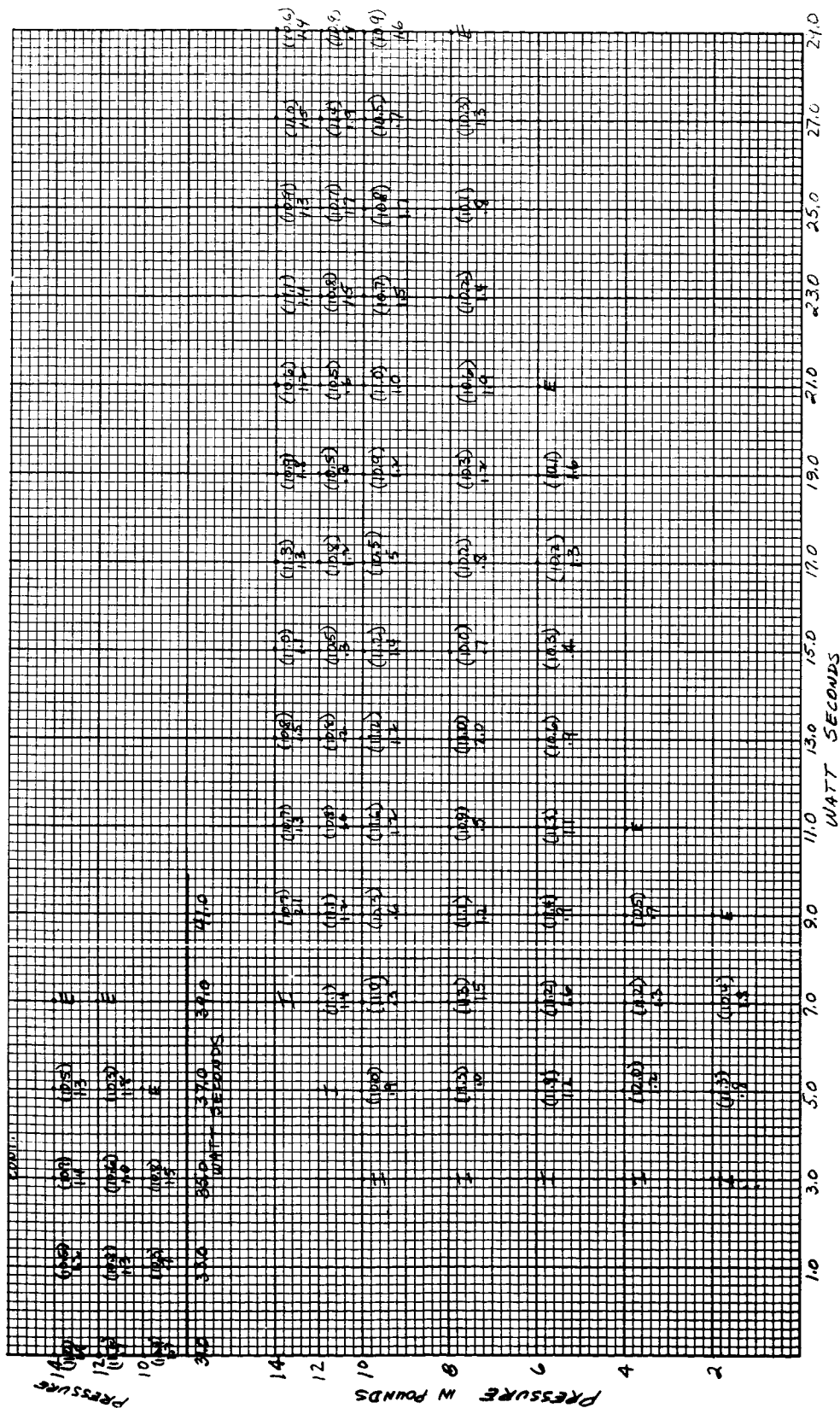


Figure 14. Isostrength Diagram, 0.020 Inch Gold Plated Nickel Wire to 0.010 to 0.020 Inch Bare Nickel Ribbon, Slope 1

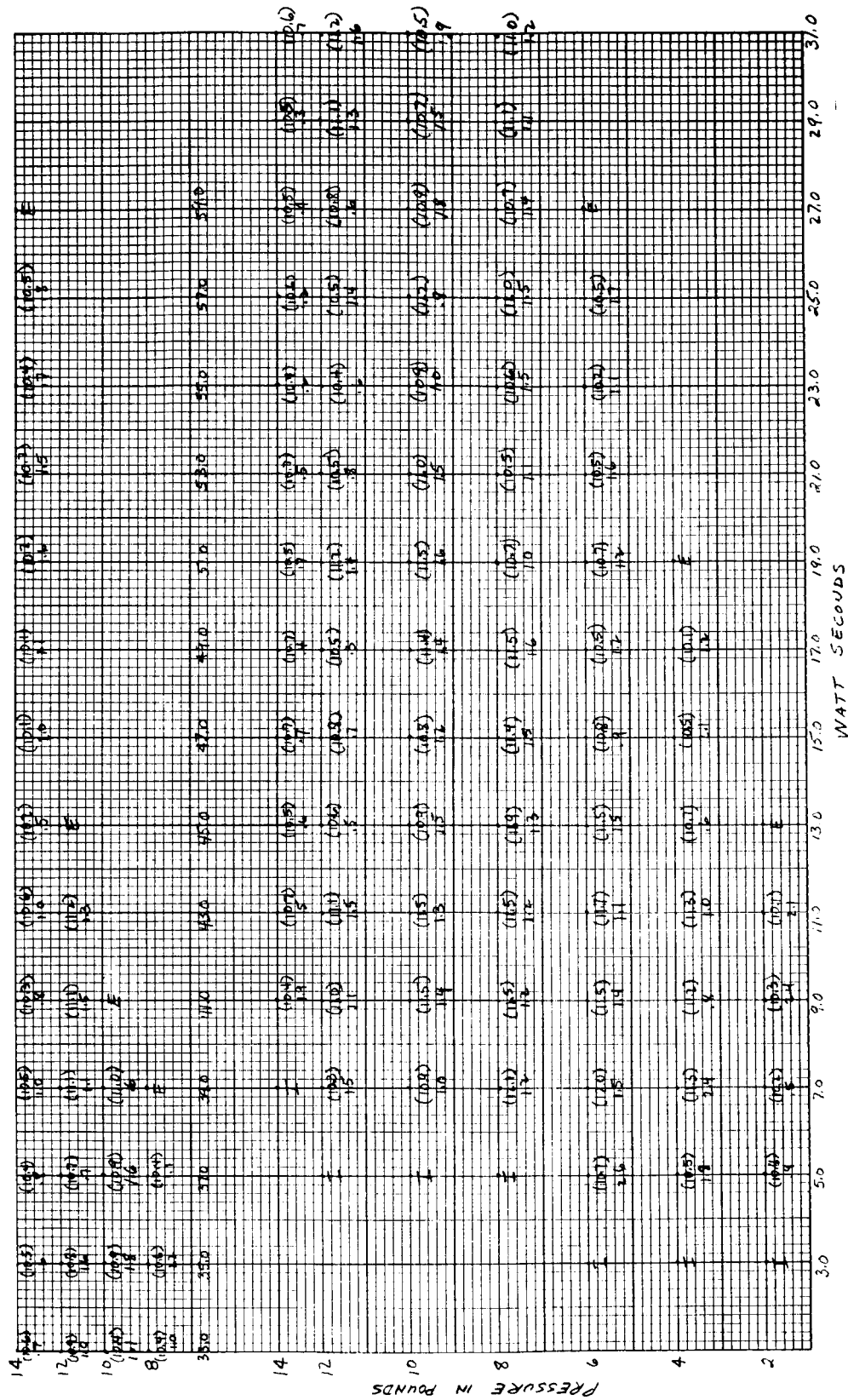


Figure 15. Isostrength Diagram, 0.020 Inch Gold Plated Nickel Wire to 0.010 by 0.020 Inch Bare Nickel Ribbon, Slope 6

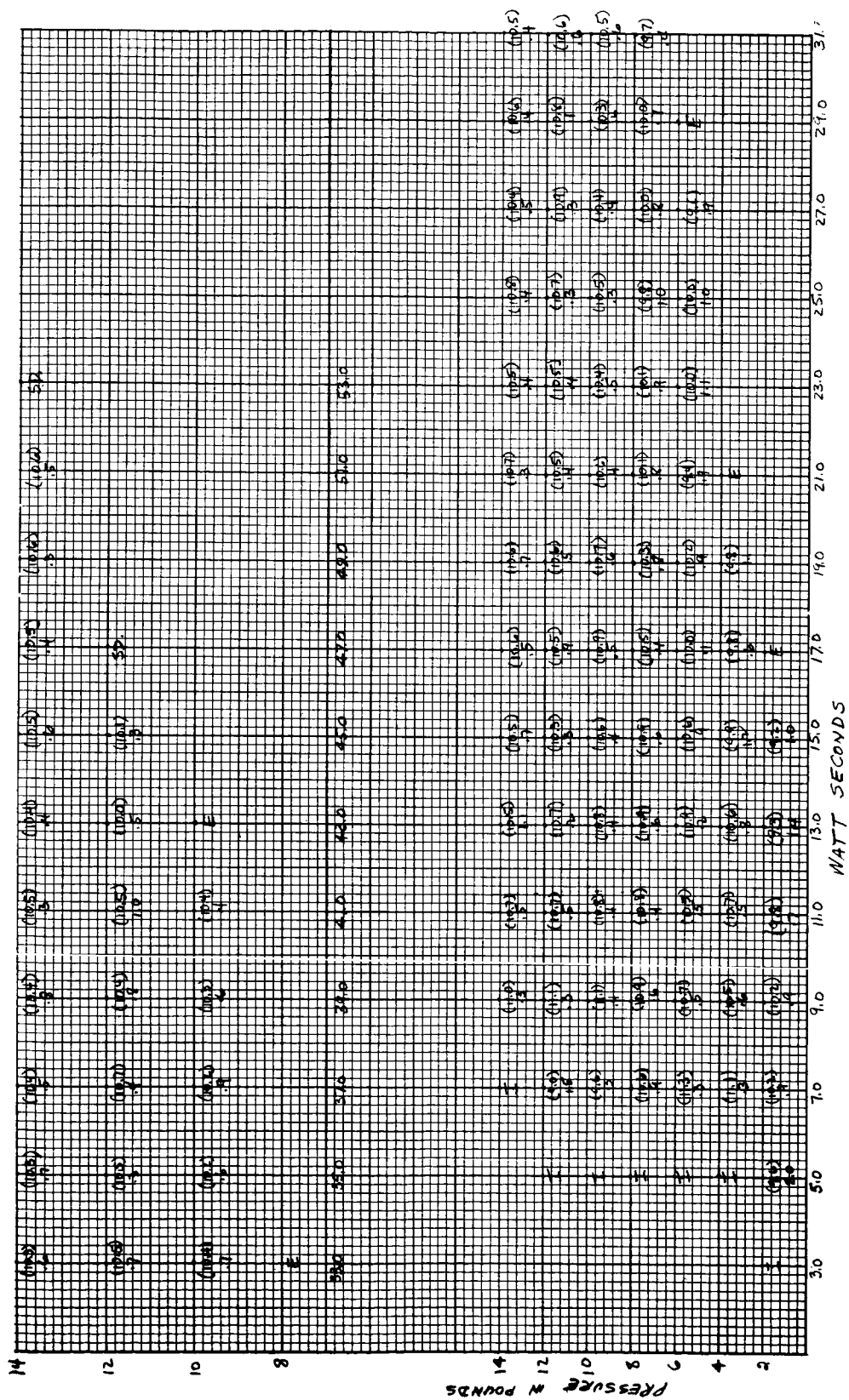


Figure 16. Isostrength Diagram, 0.020 Inch Gold Plated Nickel Wire to 0.010 by 0.020 Inch Bare Nickel Ribbon, Slope 12

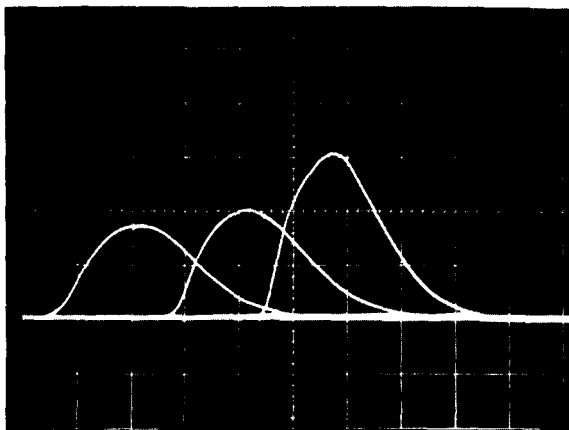


Figure 17. Weld Pulse Rise Time, Slopes 12, 6, and 1 (Left to Right)

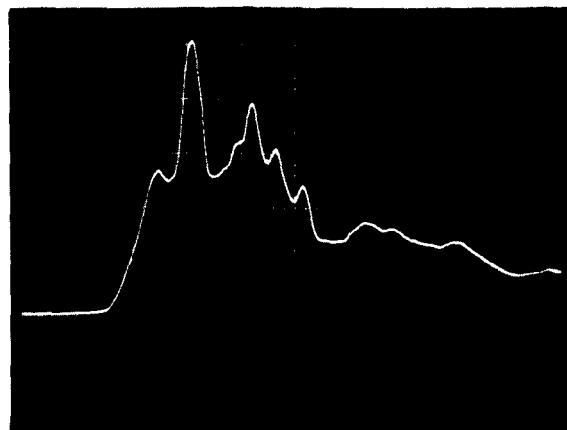


Figure 18. Weld Explosion

Figures 19 through 24 are isostrength diagrams for the remaining Dumet and Kovar gold plated lead materials. By using an established procedure, the optimum welding parameters were selected from the data contained in the isostrength diagrams and are shown in Table V as compared with the IR data.

TABLE V

Optimum Parameters Based On Isostrength Data

Material	Slope No.	Welder Pressure (lb)	Welder Energy (WS)	Avg IR Output (mV)	IR Data Spread (mV)
0.017 inch diameter Kovar (gold plated)	1	6	3.0	386	360-430
	6	4	4.0	564	510-590
	12	6	4.0	752	650-830
0.020 inch diameter Nickel (gold plated)	1	10	13.0	328	310-360
	6	10	17.0	380	330-460
	12	10	17.0	-	-
0.020 inch diameter Dumet (gold plated)	1	10	7.0	181	130-240
	6	6	8.0	222	150-285
	12	6	8.0	249	140-300

This method of selecting optimum parameters employs the use of the largest possible area encompassing acceptable welds. The optimum point is centrally located in this rectangle. When comparing results in Table V

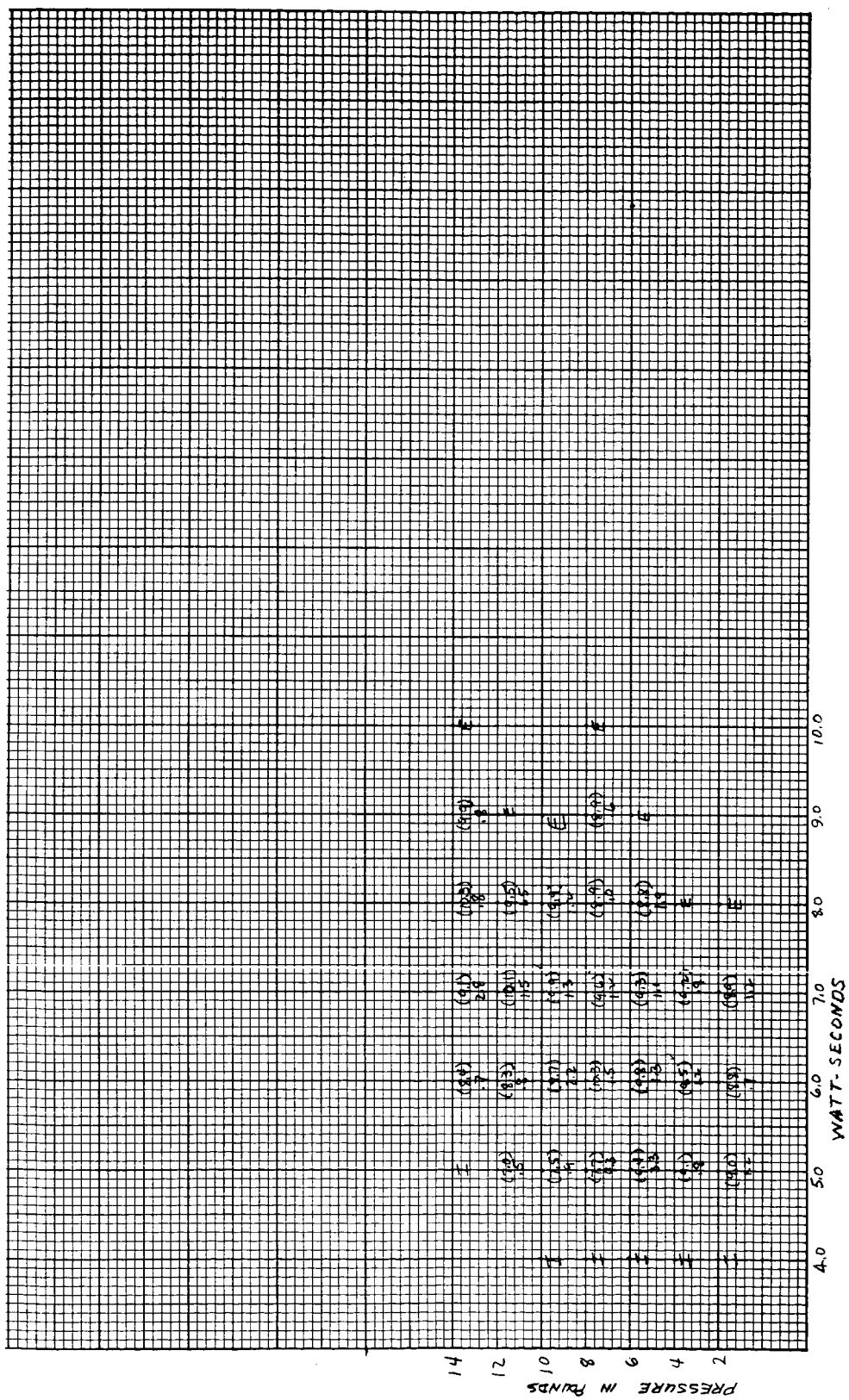


Figure 19. Isostrength Diagram, 0.020 Inch Gold Plated Dumet Wire to 0.010 by 0.020 Inch Bare Nickel Ribbon, Slope 1

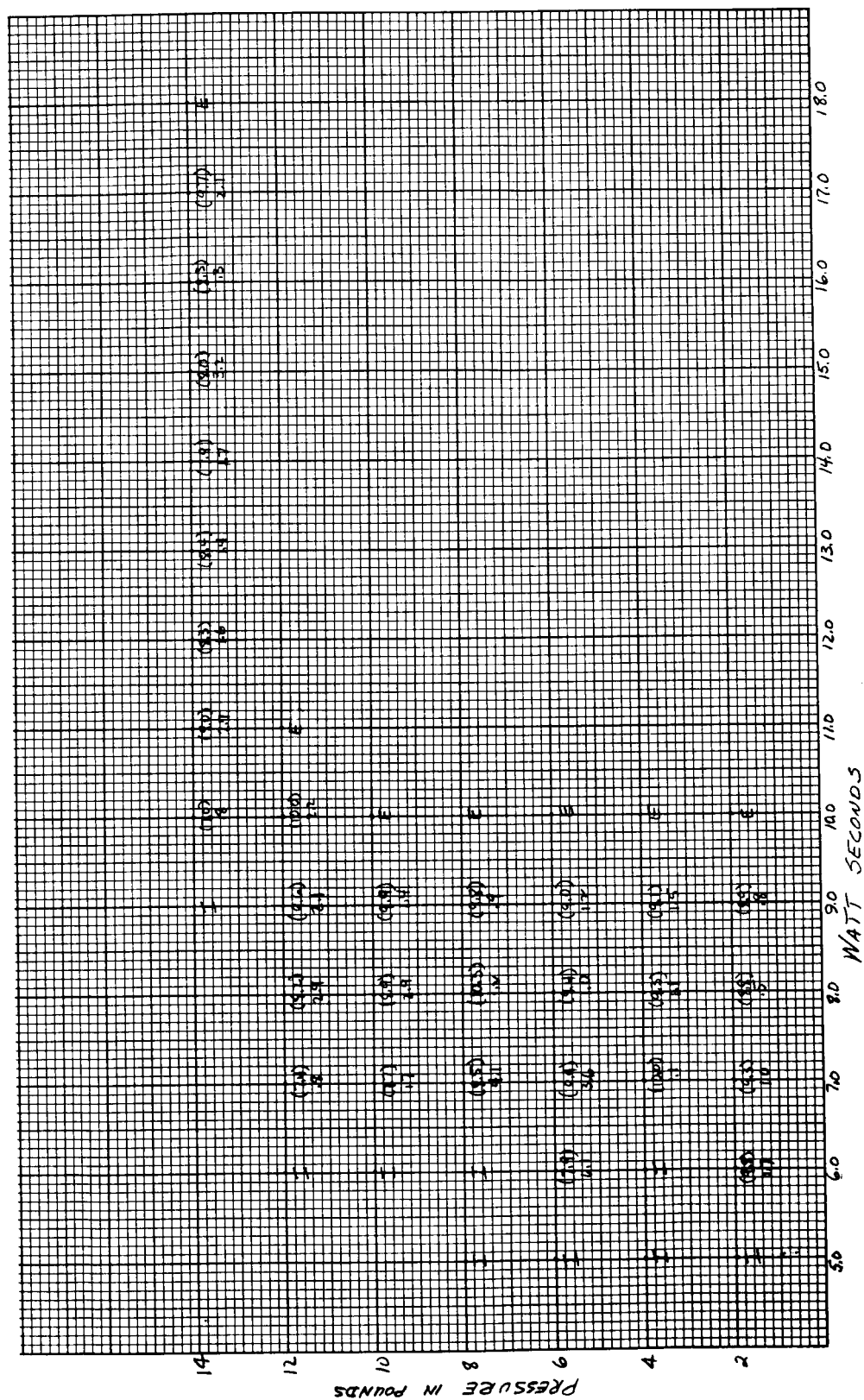


Figure 20. Isostrength Diagram, 0.020 Inch Gold Plated Dumet Wire to
0.010 by 0.020 Inch Bare Nickel Ribbon, Slope 6

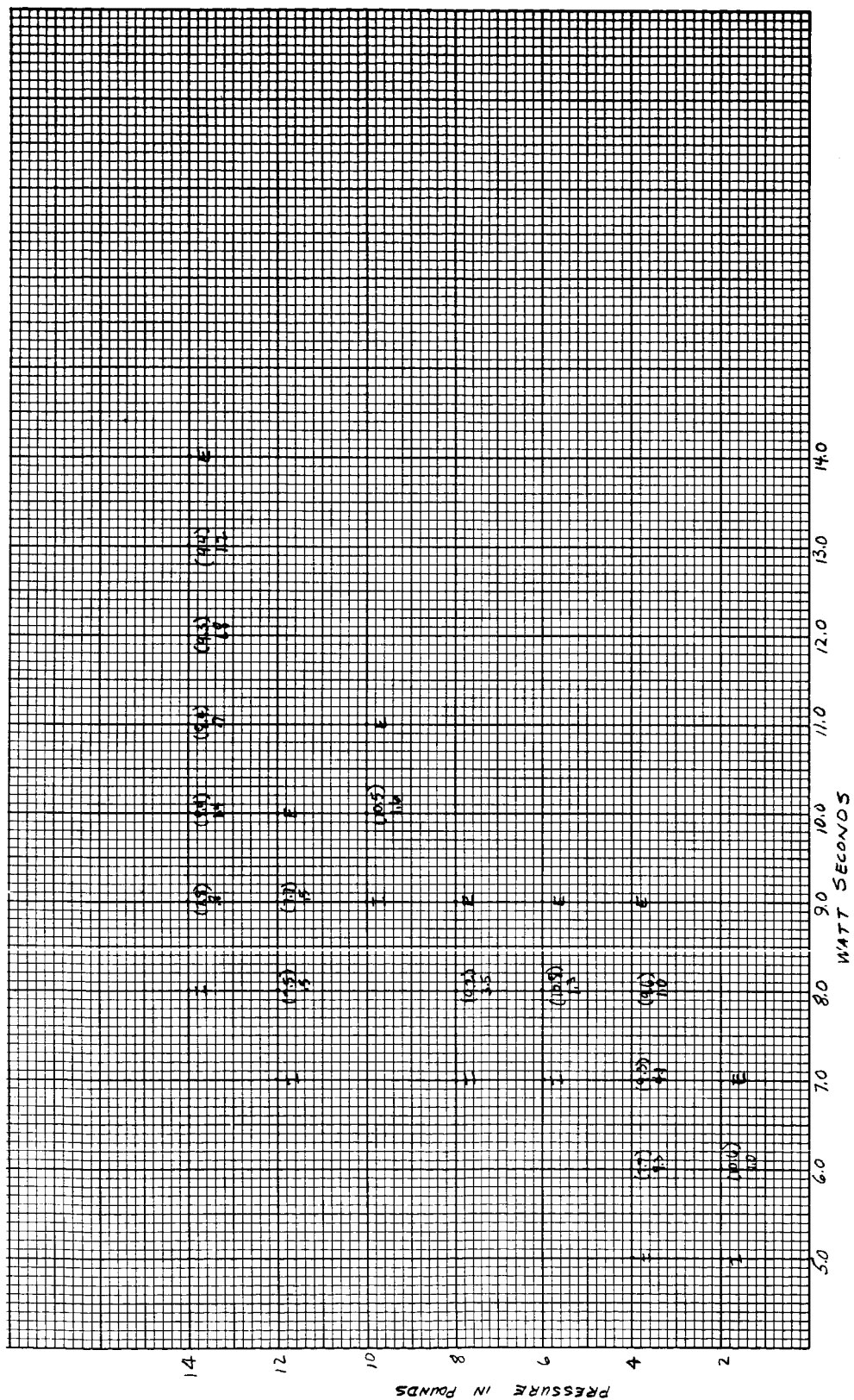


Figure 21. Isostrength Diagram, 0.020 Inch Gold Plated Dumet Wire to 0.010 by 0.020 Inch Bare Nickel Ribbon, Slope 12

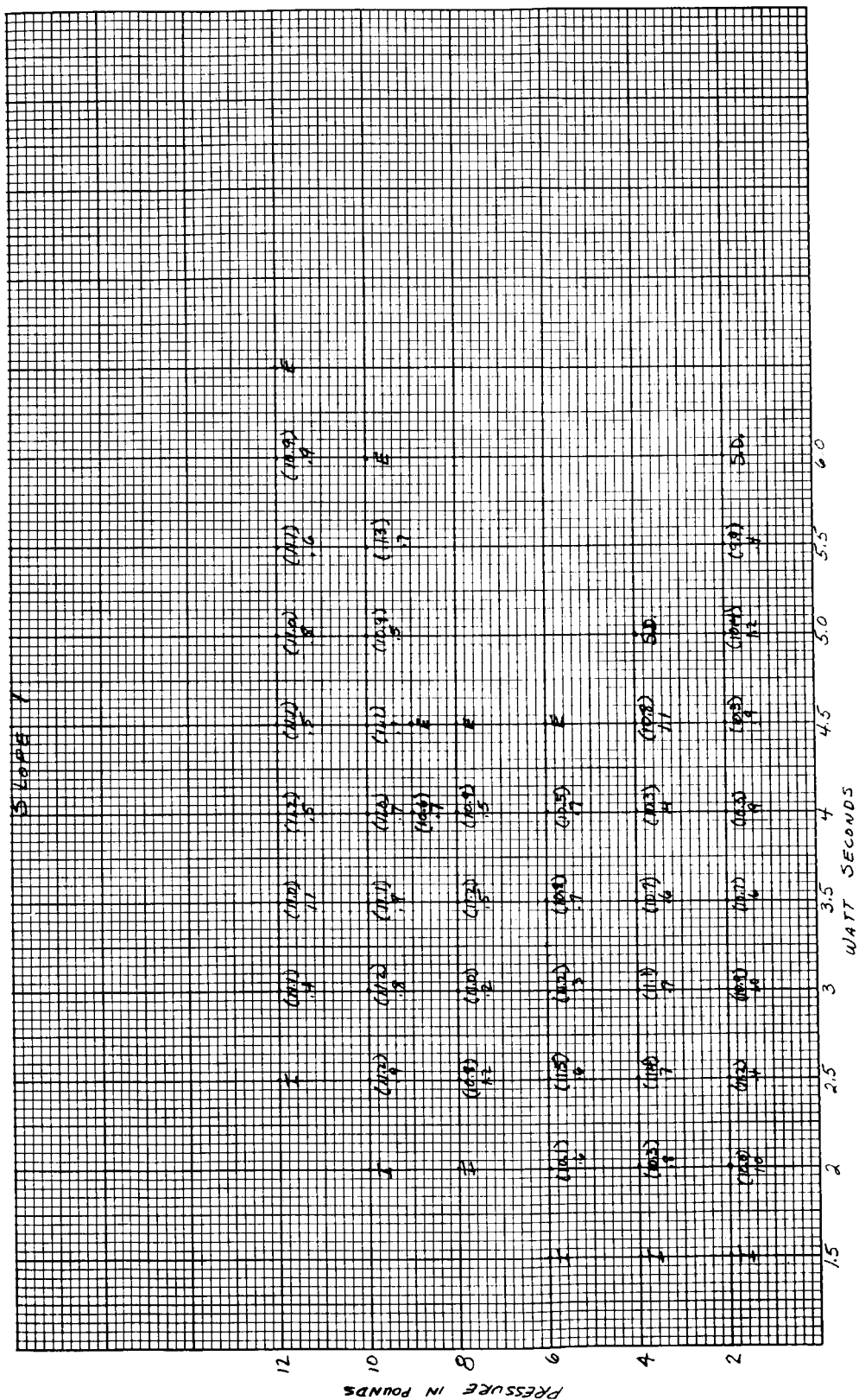


Figure 22. Isostrength Diagram, 0.017 Inch Gold Plated Kovar Wire to 0.010 by 0.020 Inch Bare Nickel Ribbon, Slope 1

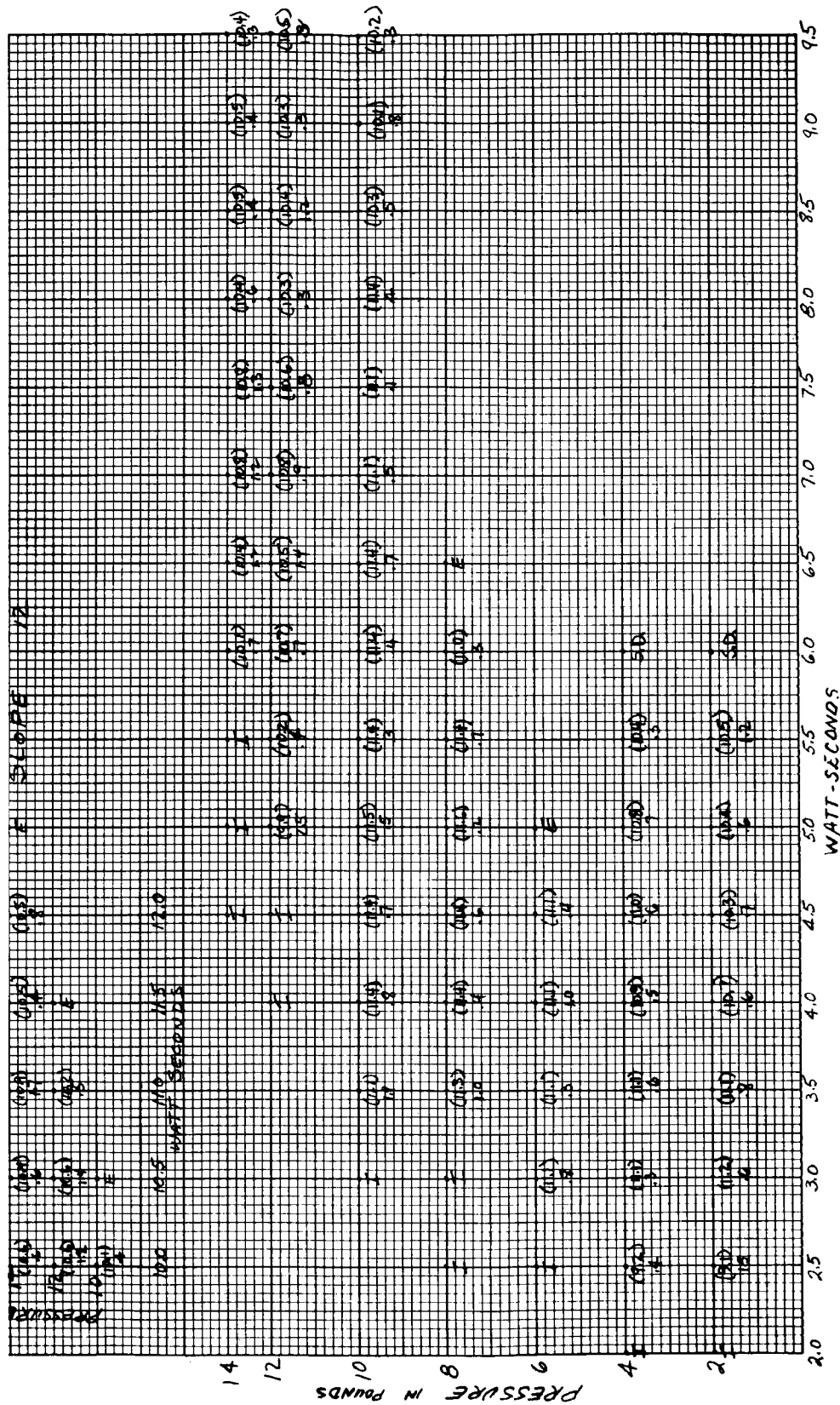


Figure 24. Isostrength Diagram, 0.017 Inch Gold Plated Kovar Wire to 0.010 by 0.020 Inch Bare Nickel Ribbon, Slope 12

with the data in Tables I, II, and III, significantly lower pressures are recommended. This difference is attributable to method of evaluation, area versus single pressure concept. However, the IR data spread in Table IV is within the IR range known to produce acceptable welds as shown in Tables I, II, and III.

Since the OFHC Copper lead material proved to be unweldable, evaluation of the results is not presented in this report. Low strength welds were characterized by evidence of weld "spitting" or minor expulsion.

A metallographic study has been made for the material combinations considered in this program. Figure 25 shows a general view of the metallography laboratory, with the metallograph located in the center background, bench binocular microscopes in the center foreground, and sample polish-

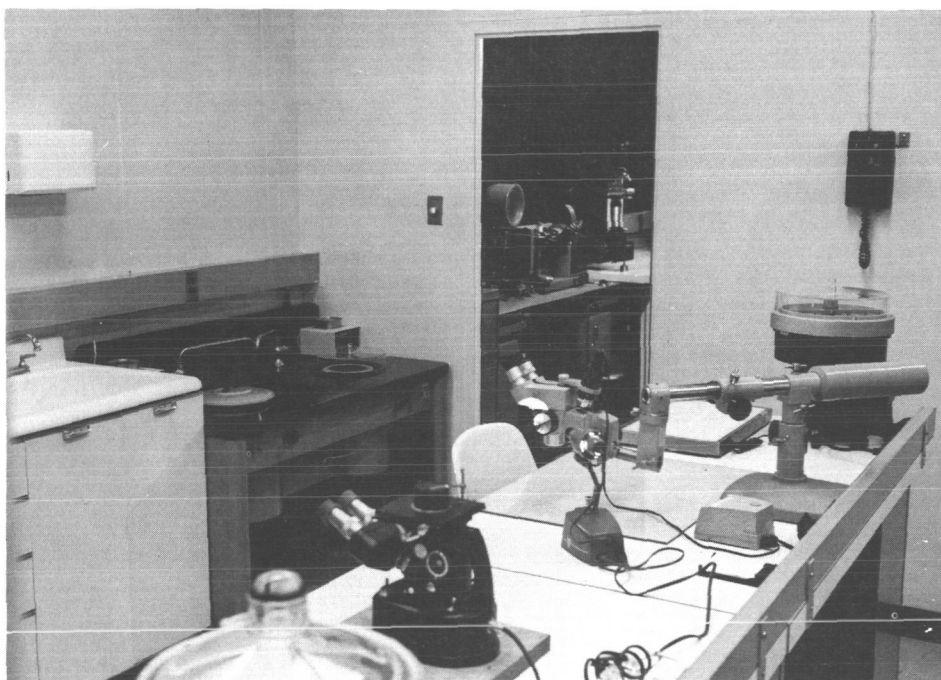
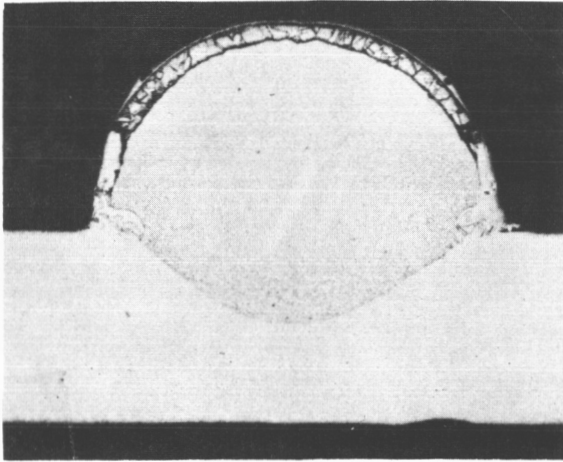


Figure 25. Metallography Laboratory

ing equipment in the left center of the photograph. Photomicrographs of the welds in both the bare and gold plated surface conditions are shown in Figures 26 through 28. The welds were made using the weld strength-IR knowledge gained during this contract. Parameters were selected that would result in welds in the:

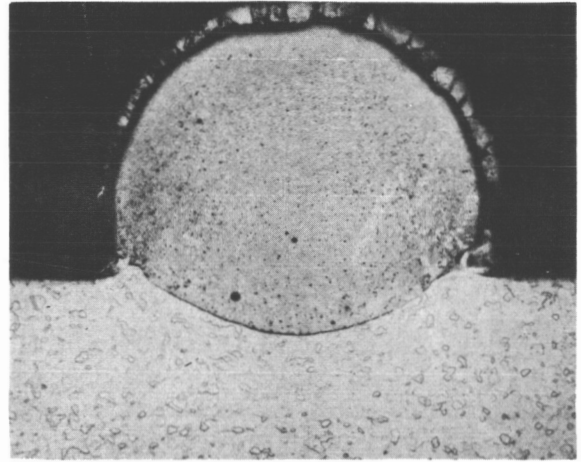
- 1 Lower no-go range or low strength weld

Gold Plated Wire

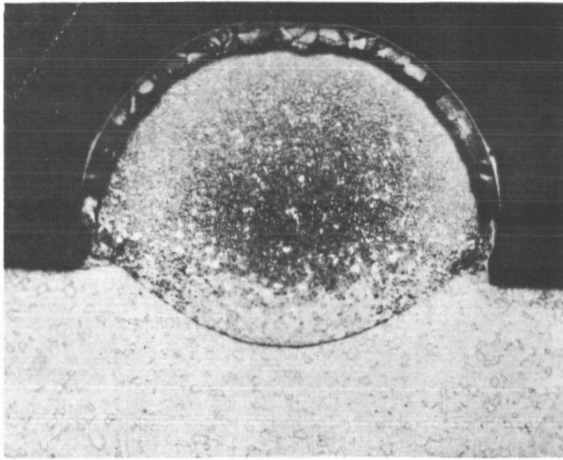


(a) HI, NO-GO Range

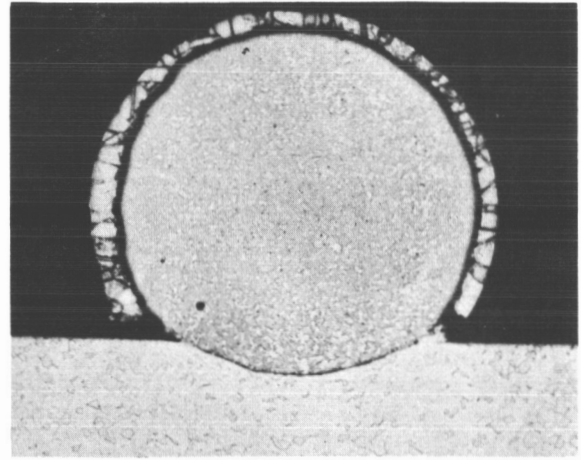
Bare Wire



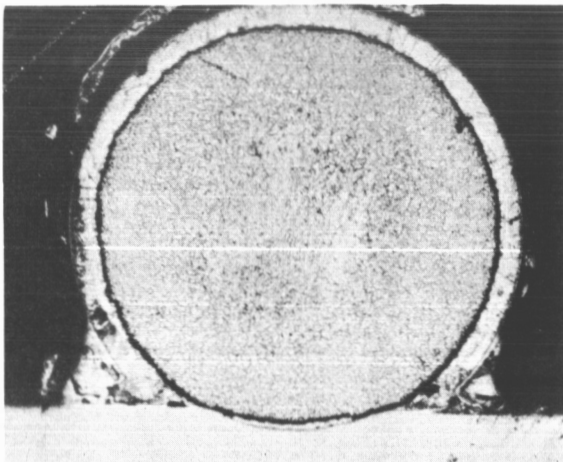
(a) HI, NO-GO Range



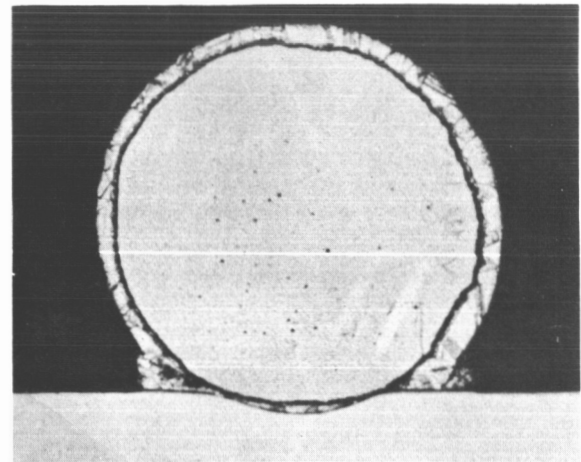
(b) GO Range



(b) GO Range



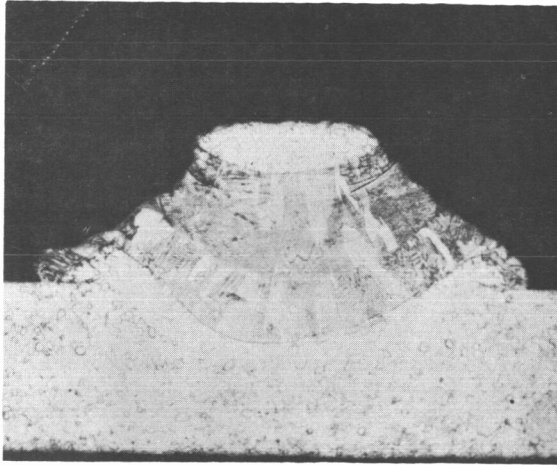
(c) LO, NO-GO Range



(c) LO, NO-GO Range

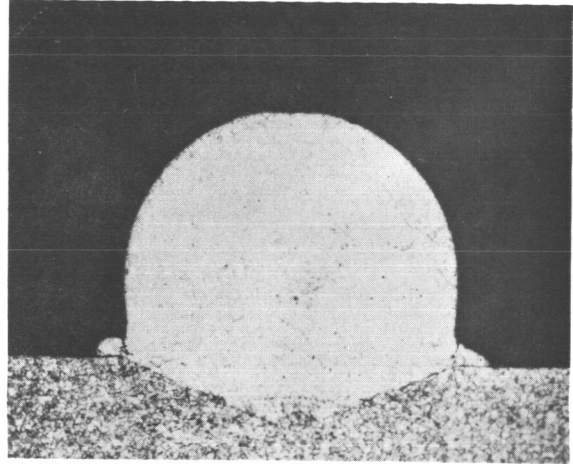
Figure 26. 0.020 Inch Dumet Wire Welded to 0.010 by 0.020 Inch Bare Nickel Ribbon

Gold Plated Wire

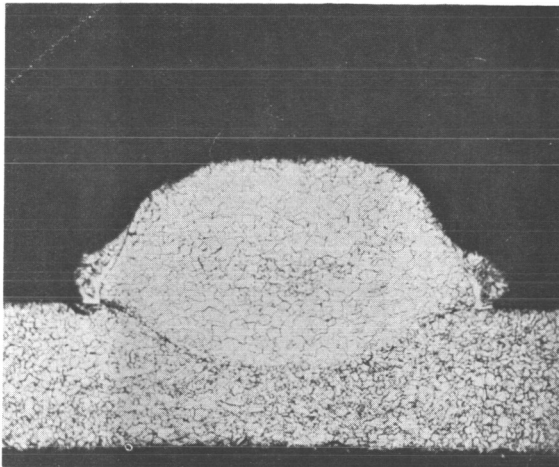


(a) HI, NO-GO Range

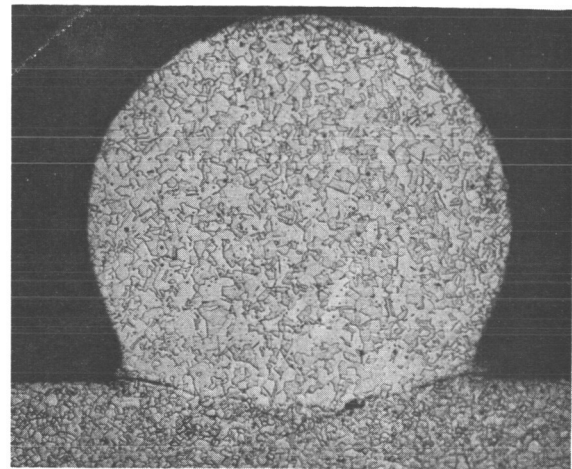
Bare Wire



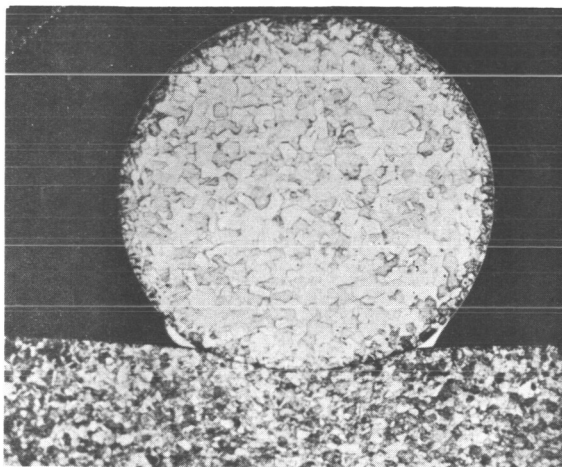
(a) HI, NO-GO Range



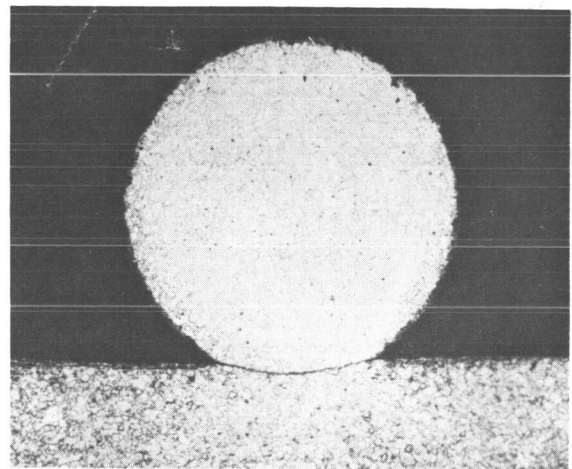
(b) GO Range



(b) GO Range



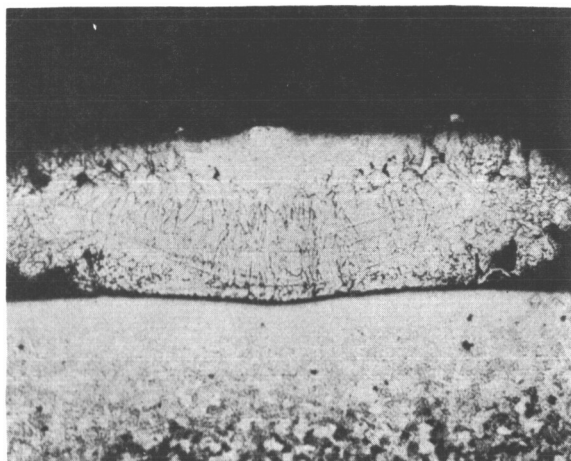
(c) LO, NO-GO Range



(c) LO, NO-GO Range

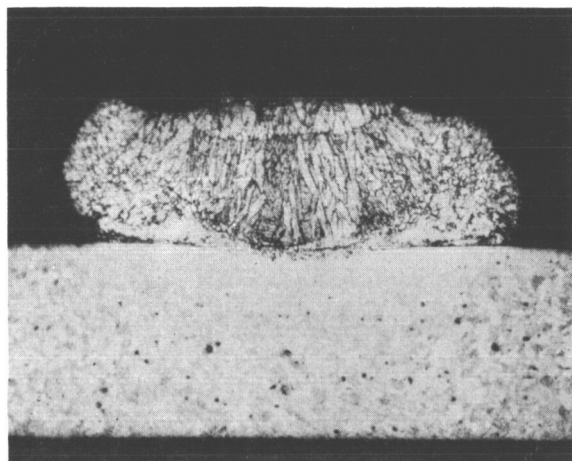
Figure 27. 0.020 Inch Nickel Wire Welded to 0.010 to 0.020 Inch Bare Nickel Ribbon

Gold Plated Wire

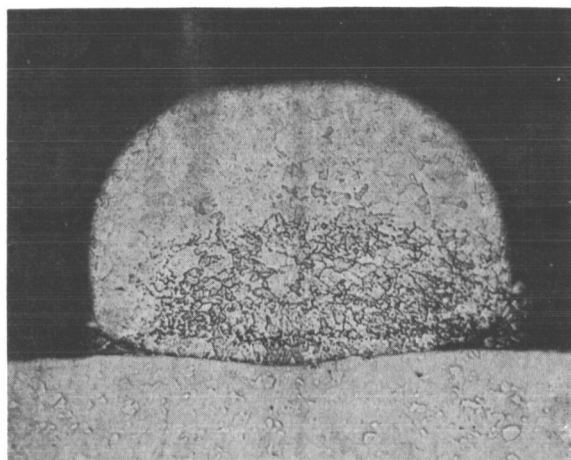


(a) HI, NO-GO Range

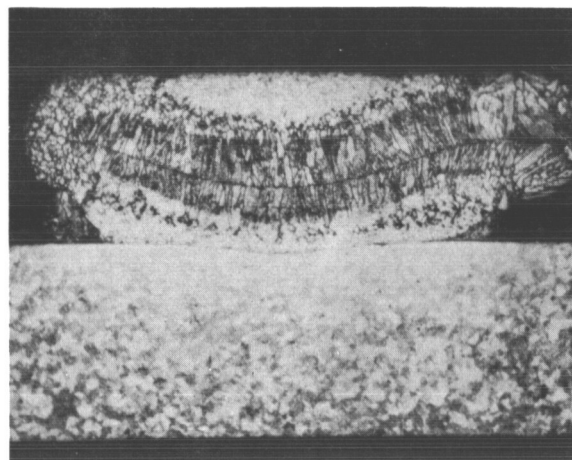
Bare Wire



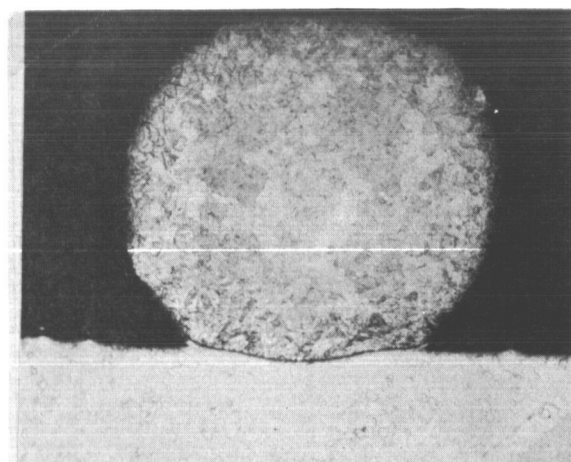
(a) HI, NO-GO Range



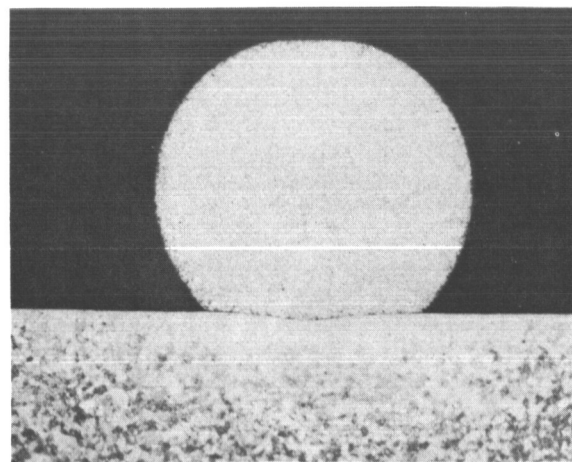
(b) GO Range



(b) GO Range



(c) LO, NO-GO Range



(c) LO, NO-GO Range

Figure 28. 0.017 Inch Kovar Wire Welded to 0.010 by 0.020 Inch Bare Nickel Ribbon

2 Go range or optimum parameters weld

3 Higher no-go range or welds showing expulsion.

The welds were sectioned and polished to the midpoint of the joint. In all cases the lead material will appear as the upper member with the nickel ribbon the lower.

An attempt was made to preserve the edge of the specimen in order to show the thin (50×10^{-6} inches) gold plating around the periphery of the lead wires as well as the copper sheath on the Dumet wire. In the low no-go range all samples show incomplete fusion with only a mechanical bond evident. In Dumet lead material, the force applied to the lead-ribbon joint by the welder has caused the copper sheath to exude and remain unmelted at the edge of the weld. Photographs of the go range show generally improved penetration with grain growth across the lead-ribbon interface evident in the Nickel (bare and gold plated) and gold plated Dumet material combinations only. Although increased penetration was seen on the bare Dumet lead sample, grain growth was not evident. The weld strength however was acceptable and within the range for gold plated Dumet lead material. It can be seen in Figure 28 for Kovar lead material, that the penetration was not improved by increasing the welder energy but rather the Kovar wire was compressed. Thus the improved weld strength is attributed to the increase in surface contact area rather than improved metallurgical bonding. This sample also shows the weld nugget to be centered in the Kovar material rather than the lead-ribbon interface. Further investigation showed that it was possible to improve the location of the weld nugget by reversing the lead-ribbon orientation. Selection of special welding electrodes or additional manipulation of welder electrodes should center the weld nugget as shown in Figure 29.

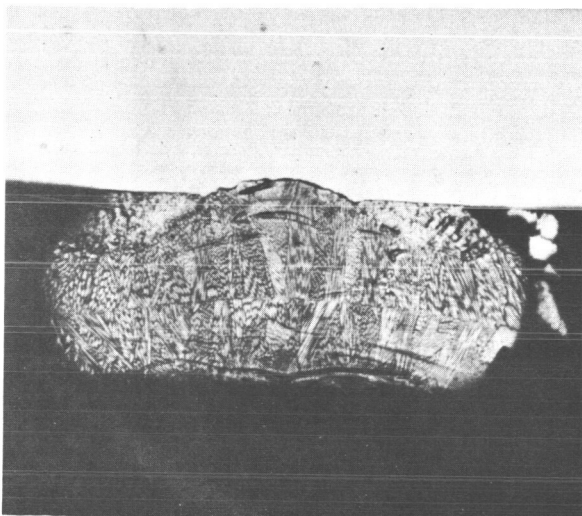


Figure 29. Kovar Wire Weld, Lead Ribbon Orientation Reversed

The high no-go range is characterized by deformed welds or expulsion. Even though the extreme energy levels were used, complete fusion has not occurred in the bare Dumet lead sample. At these higher energy levels, incipient melting and alloying of the copper sheath with the lead material can be seen in the gold plated Dumet weld photomicrograph (Figure 26).

2. Other Variables

Experiments were also performed with variables that can deteriorate weld quality. These variables include:

- 1 Surface Condition - Contamination of leads with grease, lipstick, oxides, etc., had a marked effect on the IR output; however, the weld strength was not reduced. The IR range became quite erratic when contaminant was introduced.
- 2 Alignment - The position of the lead-ribbon combination on the face of the welder electrodes did not alter the weld strength although the IR output became erratic when varied from center.
- 3 Sizes - Comparison of the 0.032 diameter to 0.020 diameter lead wires showed that the use of a larger diameter wire increased the weldability range. The weld strength, although above the minimum acceptance level, was not as great for the larger diameter wire.
- 4 Position - Investigation showed that the detector, in order to give reproducible results, had to be centered on a 1/8 inch diameter spot. Because of the required sensitivity, the detector was anchored in a permanently placed holder.

II. GO, NO-GO VISUAL INDICATOR

The GO, NO-GO visual indicator (Figures 30 through 32) was designed and built to implement the infrared concept. Its functions are to: 1) sense the IR generated at the weld joint; 2) analyze the level of IR radiated; and 3) provide a GO or NO-GO indication by energizing one of three lamps. The lamps are referred to as LO, NO-GO; GO, and HI, NO-GO which are red, green, and red respectively.

Three IR curves resulting from three separate weld pulses when welding 0.017 gold-plated Kovar wire to 0.010 by 0.020 Nickel ribbon are shown in Figure 33. The smallest curve on the left is a typical LO, NO-GO curve indicating an insufficient energy level. The middle curve is a typical GO curve indicating an acceptable energy level. The largest curve on the right with the jagged top and spurt indication is typical of HI, NO-GO expulsion curves. The GO, NO-GO visual indicator is adjusted for a Kovar-to-nickel combination to indicate a GO condition for any IR curve between the limits of 0.240 volts and 1.030 volts.

The GO, NO-GO visual indicator is adjustable for any given wire combination as determined from an IR-tensile strength correlation graph for the desired wire combination.

A. SYSTEM REQUIREMENTS

The GO, NO-GO visual indicator is required to relate from the magnitude of the IR generated at the weld whether the weld is acceptable or not acceptable. Nonacceptable welds occur when too little or too much energy is used and acceptable welds occur when the energy level is within the proper range. Since the visual indicator is operated from only the IR source it is necessary to have three channels of evaluation. One channel to indicate the correct amount of energy for acceptable welds and two channels to indicate too little or too much energy for nonacceptable welds.

1. Voltage Level Detection

The magnitude of a voltage waveform, as a translation of the IR pulse, is evaluated by differential amplifiers.

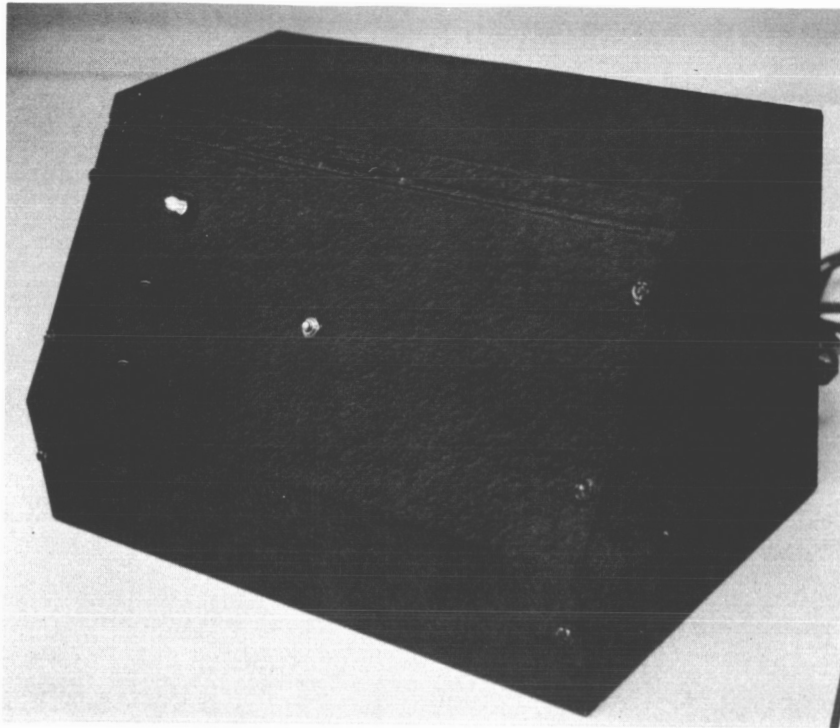


Figure 30. GO, NO-GO Visual Indicator

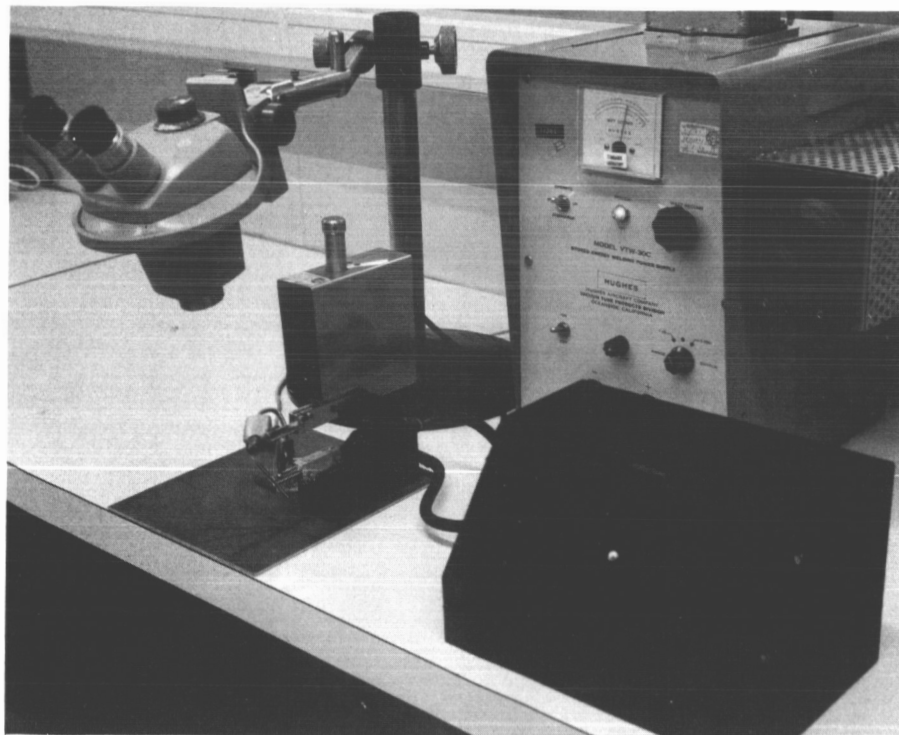


Figure 31. GO, NO-GO Test Equipment

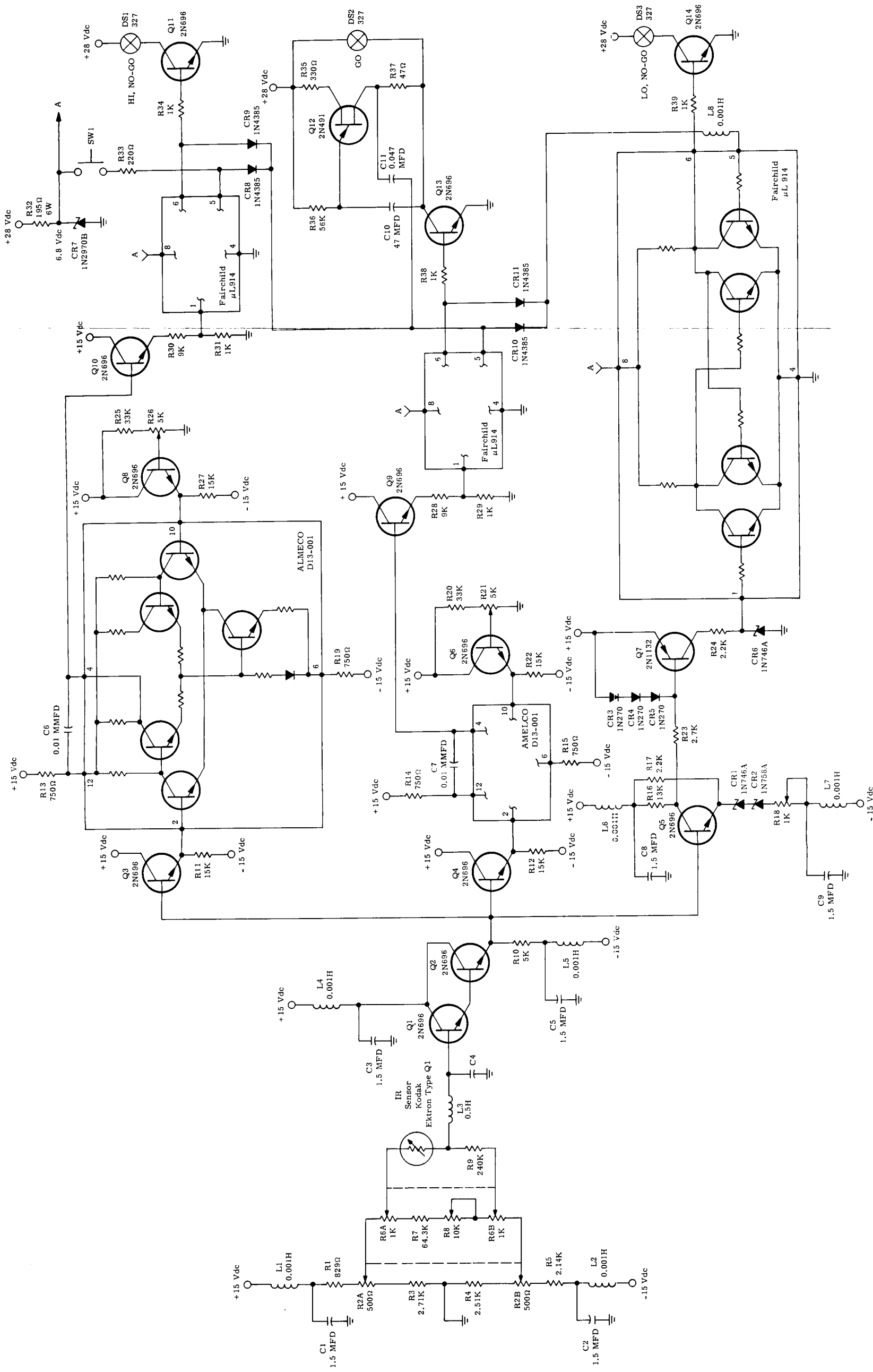


Figure 32. GO, NO-GO Visual Indicator Schematic

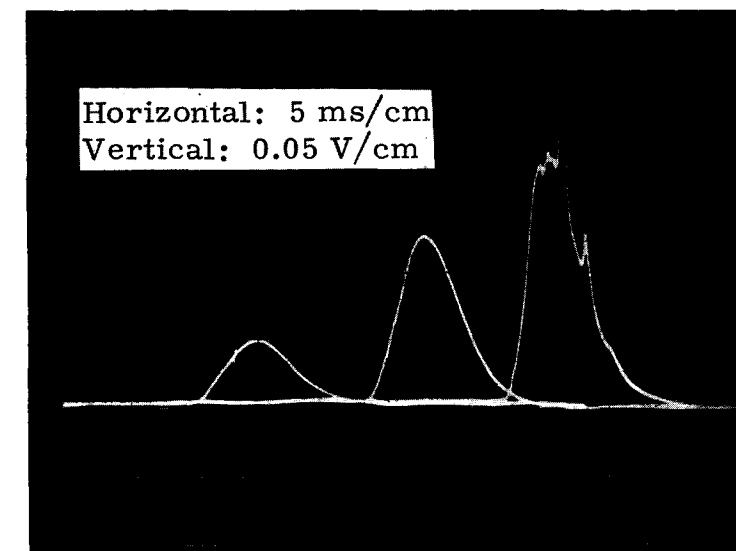


Figure 33. Three Infrared Radiation Curves
Resulting from Three Separate Weld
Pulses, Kovar Wire

a. Variable Level Set

1) LO, NO-GO

The LO, NO-GO level set should be as low as possible but still set slightly above the ambient noise level of the system. The voltage level set is 0.065 volts although the magnitude of this voltage can be varied. Once set for a given system it remains fixed for all combinations of weld material.

2) GO/HI, NO-GO

The GO and HI, NO-GO level sets are variable to accommodate the criteria of acceptable welds for all combinations of weld material. The voltage level set for GO and HI, NO-GO level is determined from the IR tensile strength correlation graph for each weld material combination.

b. Sensitivity

The visual indicator does not amplify the signal generated by the IR sensor. In fact it is attenuated by emitter-followers for isolation. The sensitivity of the visual indicator lies in the ability of the differential amplifier to trigger the memory module with a minimum differential signal

change. Although the gain of the differential amplifier $E_{\max} - E_{\min}$ output/ $E_{\max} - E_{\min}$ input is 410, sensitivity of the visual indicator lies in the narrow transition band where both GO and NO-GO indications occur.

The LO, NO-GO/GO transition band is 30 millivolt (Figure 34). The point of transition is 238 millivolts, therefore it is assumed that all IR voltage readings below 238 millivolts should be NO-GO and all above should be GO. All IR voltage readings are made at the infrared sensor with respect to ground. Indicator readouts at 230 millivolts had a 3 percent error and indicator readouts at 240 millivolts has a 33 percent error. There were no error readouts at 220 millivolts and below and at 250 millivolts and above.

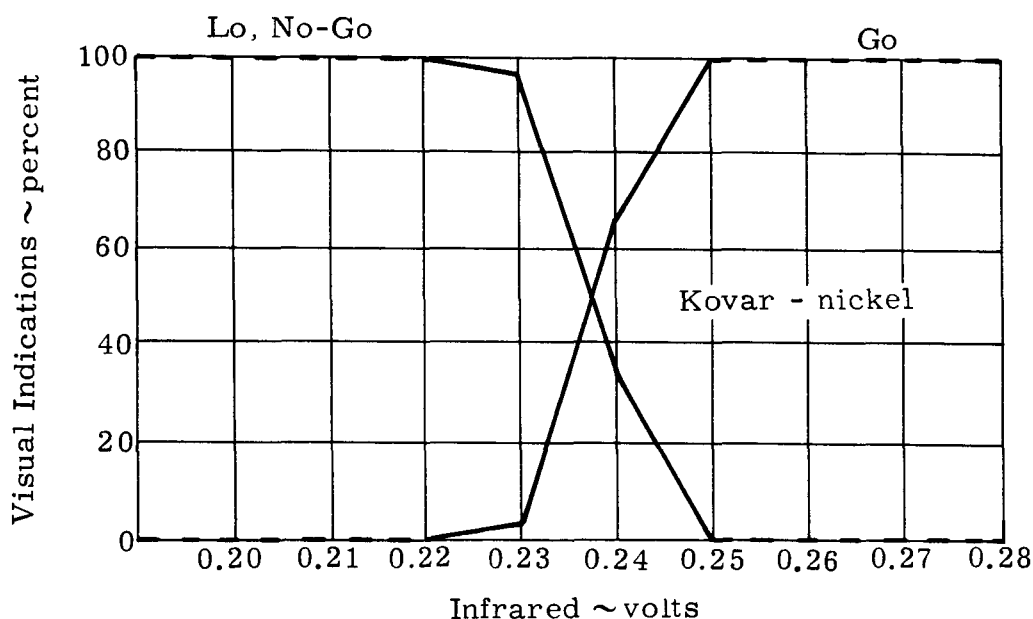


Figure 34. LO, NO-GO/GO Transition

The GO/HI, NO-GO transition band is 0.1 volts (Figure 35). The point of transition is 1.03 volts, therefore it is assumed that all IR voltage readings below 1.03 volts should be GO and all above should be NO-GO. Indicator readouts at 1.0 and 1.02 volts had a 6 percent error, at 1.04 volts a 14 percent error, and at 1.06 volts a 5 percent error. There were no errors in readouts at 0.98 volts and below and 1.08 volts and above.

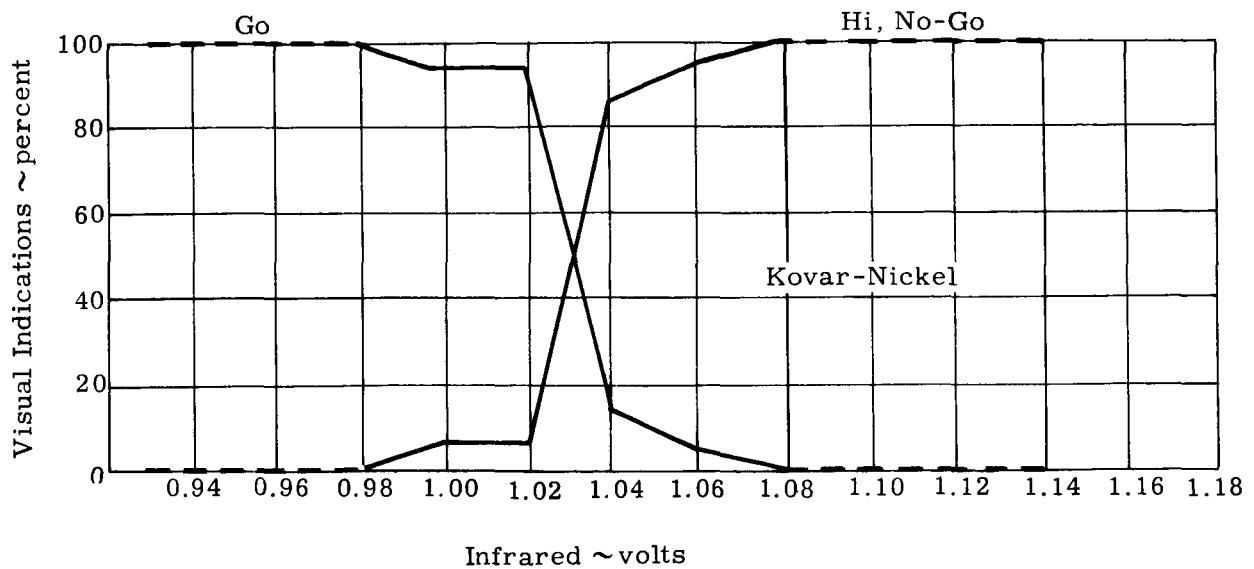


Figure 35. GO/Hi, NO-GO Transition

2. Block Diagram (Figure 36)

a. Analog

1) IR Sensor

Maximum Δ voltage/ Δ infrared occurs when the load resistor approaches the resistance of the sensor. Also it occurs when maximum rated voltage is applied to the sensor.

2) Impedance Match

A Darlington connected emitter-follower provides a very high impedance to the sensor network to reduce loading. It also provides a low impedance drive for the signal level detectors.

3) Signal Level Detector

The detector evaluates the magnitude of the generated IR and is essentially a differential amplifier whose output is triggered when the input exceeds a variable but predetermined level. The detector evaluates the magnitude of the generated IR. Three detectors are used in the visual indicator, one each for the two NO-GO channels and one for the GO channel.

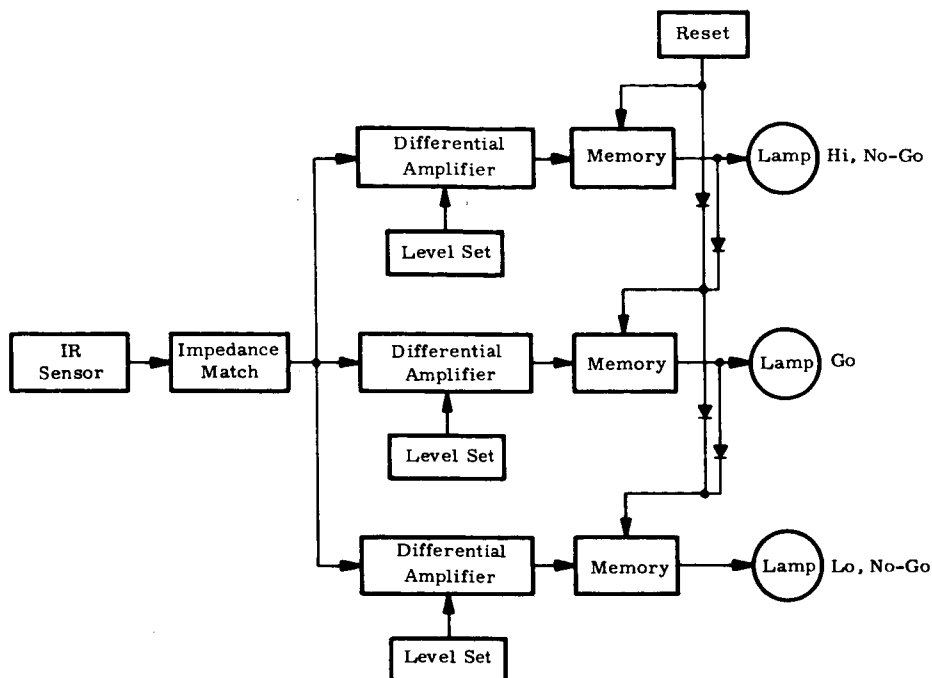


Figure 36. GO, NO-GO Visual Indicator Block Diagram

b. Digital

1) Memory and Reset

The memory modules are bistable flip-flops. Set signals from the output of the signal level detector created an output signal whereas reset signals created by operator removes the output signal.

2) Lamps

Signals from the flip-flops operate lamp drivers which control the energy to the lamps.

B. CIRCUIT DESCRIPTION

1. Infrared Sensor and Associated Circuit

Preliminary tests of IR sensors indicate that a maximum voltage change for a given IR change occurs when the load resistance equals the minimum resistance the sensor achieves in operation. Since the low levels of IR are the most difficult to detect, maximum signal (at low levels) occurs when the load resistance equals the detector dark resistance and when maximum rated voltage is applied across the sensor. Since the sensor manufacturing resistance tolerance is so large (0.2 to 1.0 megohms), it is necessary to select load resistors to match the sensor resistance.

The network to the left of the IR sensor in Figure 37 allows the maximum rated voltage to be established across the sensor by adjusting potentiometer R8. Adjusting dual potentiometers R2 and R6, where R6 is a vernier to R2, permits a zeroing of the system. Inductors L1 and L2 with capacitors C1 and C2 form a low pass filter, with the cut-off frequency of 4.1 kHz, to shunt to ground unwanted high frequency signals.

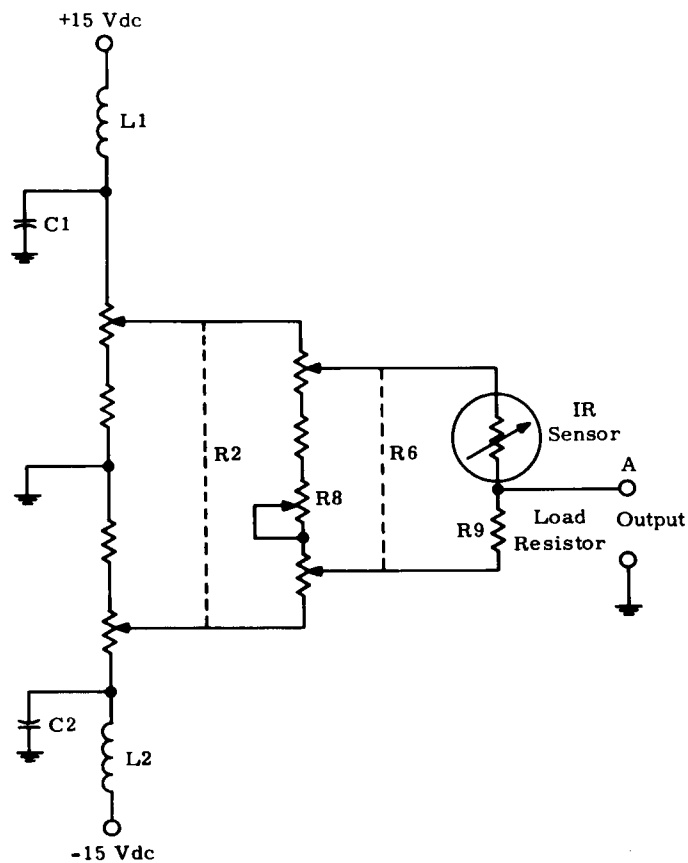


Figure 37. Infrared Detector and Associated Network

2. Darlington Circuit

The signal (A) goes through a low pass filter (Figure 38) composed of inductor L3, capacitor C4, and a cut-off frequency of 9.25 kHz, which allow only those frequencies needed to produce the signal generated by the IR sensor to pass through to the Darlington connected transistors. Therefore, the Darlington circuit assures a high impedance to the filter, to the IR sensor and load resistor. The signal is split at this point for evaluation for HI, NO-GO, GO, and LO, NO-GO, (B), (C), and (D) respectively. Zeroing the system occurs where the Darlington output is zero with respect to ground and no IR input to the sensor.

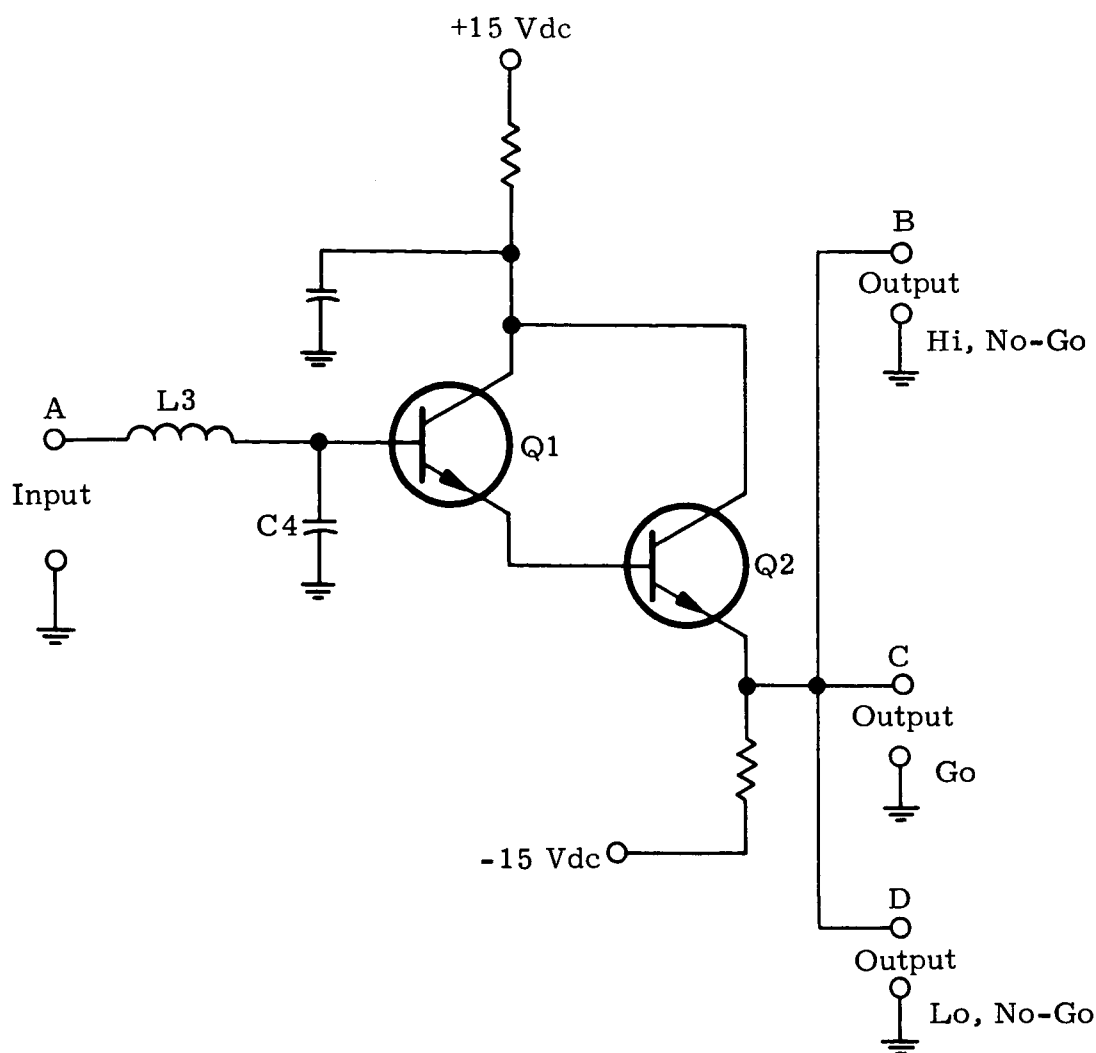


Figure 38. Impedance Matching

3. Integrated Differential Amplifiers

Signals (B) and (C) go to separate, but identical, signal level detectors (Figure 39). Signals (B) and (C) go to separate emitter followers for additional isolation and then into differential amplifiers. The voltage picked off potentiometer R26 is isolated by an emitter-follower and is used to set the voltage level at which the differential amplifier is triggered. When the signal (B) or (C) reaches the level set voltage, the output signal (E) or (F) increases from a near zero voltage to its maximum, as the input increases another 30 millivolts. Capacitor C6 suppresses RF oscillations during the output transition.

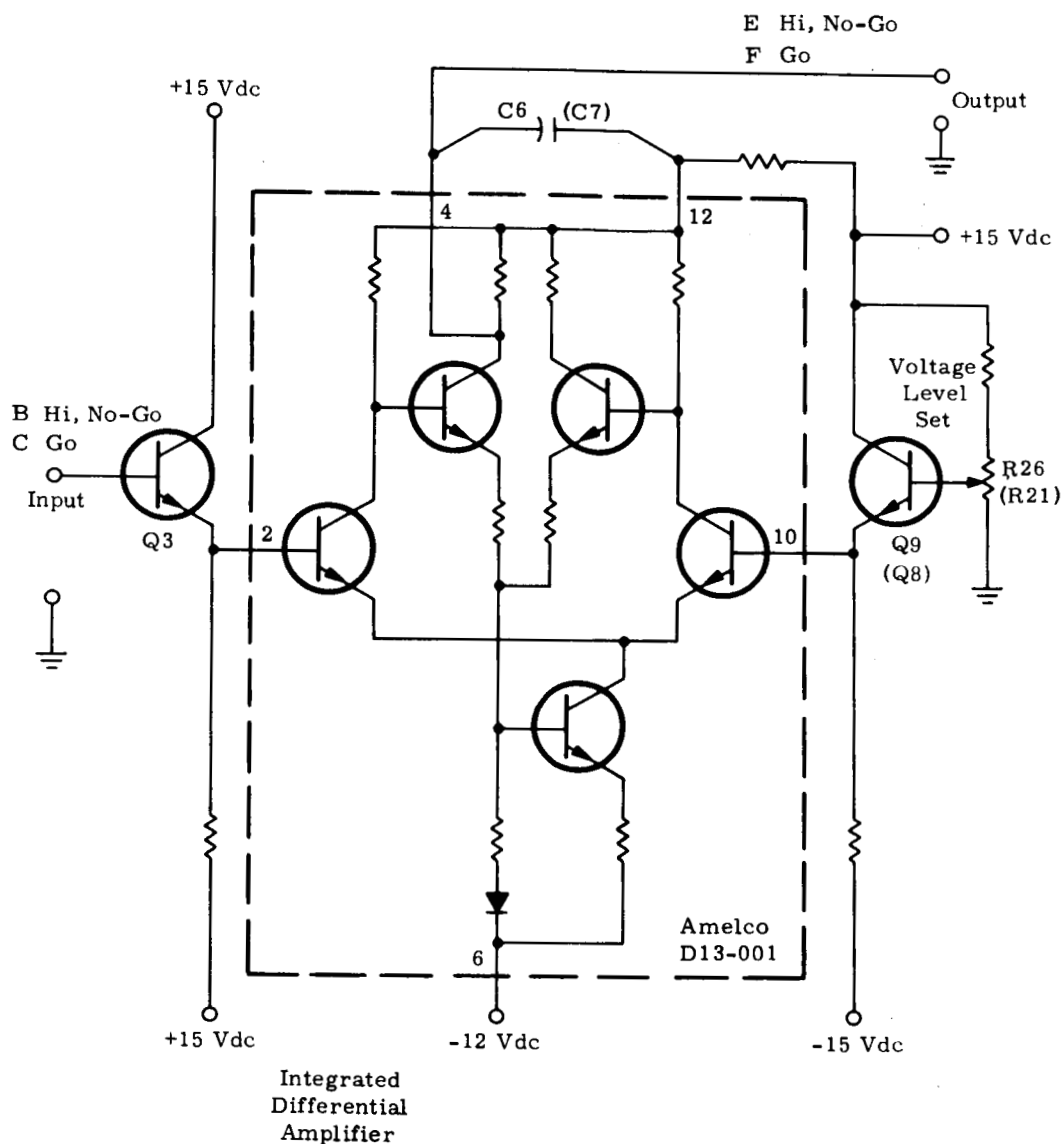


Figure 39. HI-NO-GO/GO Signal Level Detector

4. LO, NO-GO Signal Level Detector

The LO, NO-GO signal is amplified by a npn transistor circuit (Figure 40) having an adjustable fixed bias R18. Inductors L6 and L7 with capacitors C8 and C9 form a low pass filter with the cut-off frequency of 4.1 kHz to shunt to ground unwanted high frequency signals. The signal is direct coupled to a pnp transistor, Q7. Diodes CR1, CR2, and CR3 protect the transistor by limiting the magnitude of the base to emitter voltage. Resistor R24 and the resistance of the following stage form the load for transistor Q7. Zenor diode CR6 limits the current to the following stage.

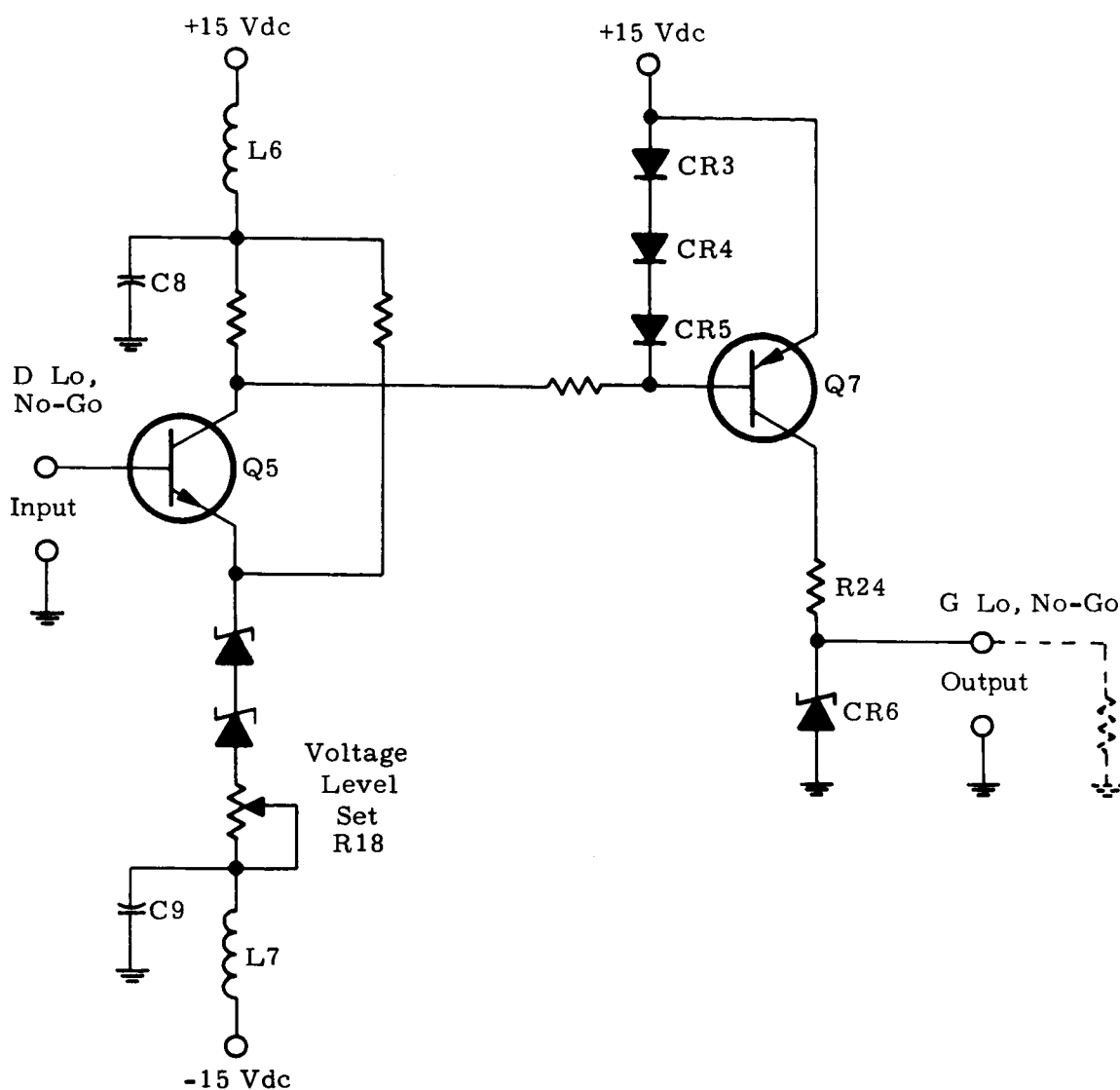


Figure 40. LO, NO-GO Signal Level Detector

5. Integrated Flip-Flop

The HI, NO-GO signal from its signal level detector is fed into an emitter-follower Q10 (Figure 41) for isolation and attenuation to trigger the flip-flop memory circuit at terminal 1. This circuit is a Fairchild μ L914 integrated circuit. The signal out at terminal 6 performs two functions: 1) causes transistor Q11 to conduct, thereby energizing a red lamp DS1, significant of a HI, NO-GO signal; and 2) furnishes a reset to the GO and LO, NO-GO memory circuit. The reset switch SW1 is closed momentarily to furnish a signal to terminal 5 of each memory circuit to reset them to their original state.

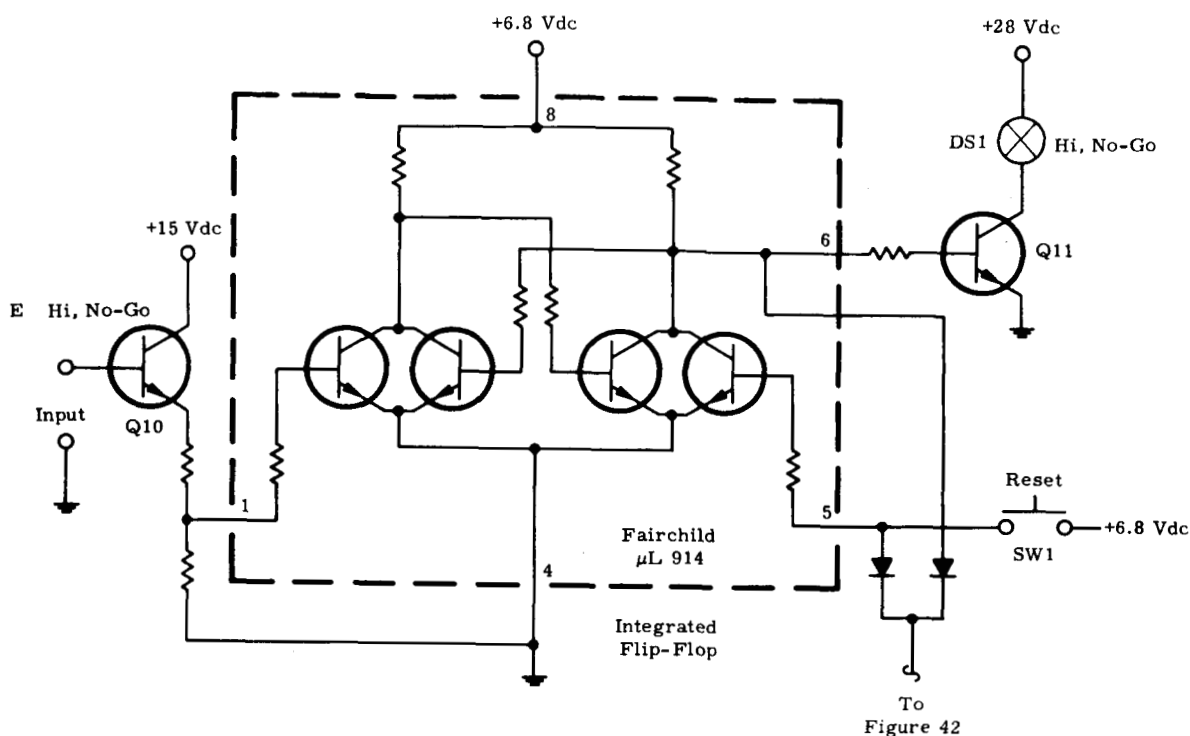


Figure 41. HI, NO-GO Memory and Reset

6. Automatic Reset Circuit

The GO signal from its signal level detector is fed into an emitter-follower Q9 (Figure 42) for isolation and attenuation to trigger the flip-flop memory circuit at terminal 1. This circuit is a Fairchild $\mu\text{L} 914$ integrated circuit. The signal out at terminal 6 performs two functions: 1) furnishes a reset to the LO, NO-GO memory circuit, 2) causes transistor Q13 to conduct thereby energizing a green lamp, significant of a GO signal, and energizing a timing circuit associated with the unijunction transistor Q12. The timing circuit contains a capacitor C10 that is charged through resistor R36. When the voltage across C10 is sufficient to cause the unijunction to conduct, a signal is generated across resistor R37 and coupled through capacitor C11 to terminal 5 of the GO and LO, NO-GO memory circuit to reset them to their original state.

7. LO, NO-GO Memory and Reset

The LO, NO-GO signal from its signal level detector triggers the flip-flop memory circuit at terminal 1 (Figure 43). This circuit is a Fairchild $\mu\text{L} 914$ integrated circuit. The signal out at terminal 6 causes transistor Q14 to conduct thereby energizing a red lamp, significant of a LO, NO-GO signal.

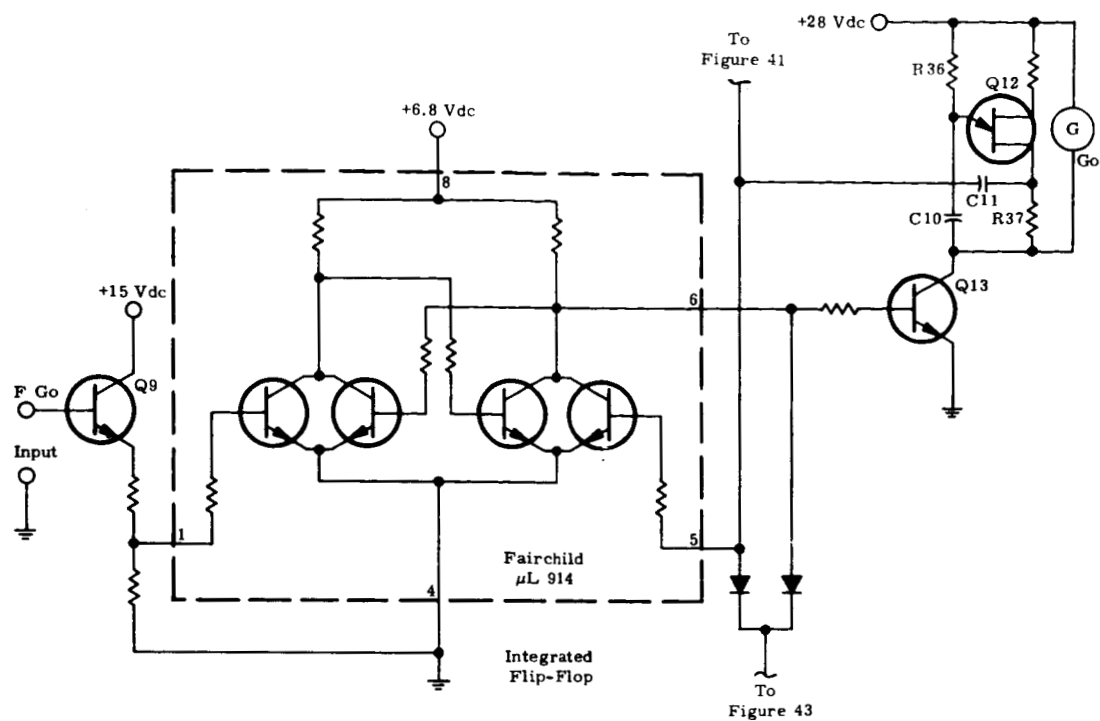


Figure 42. GO Memory and Reset

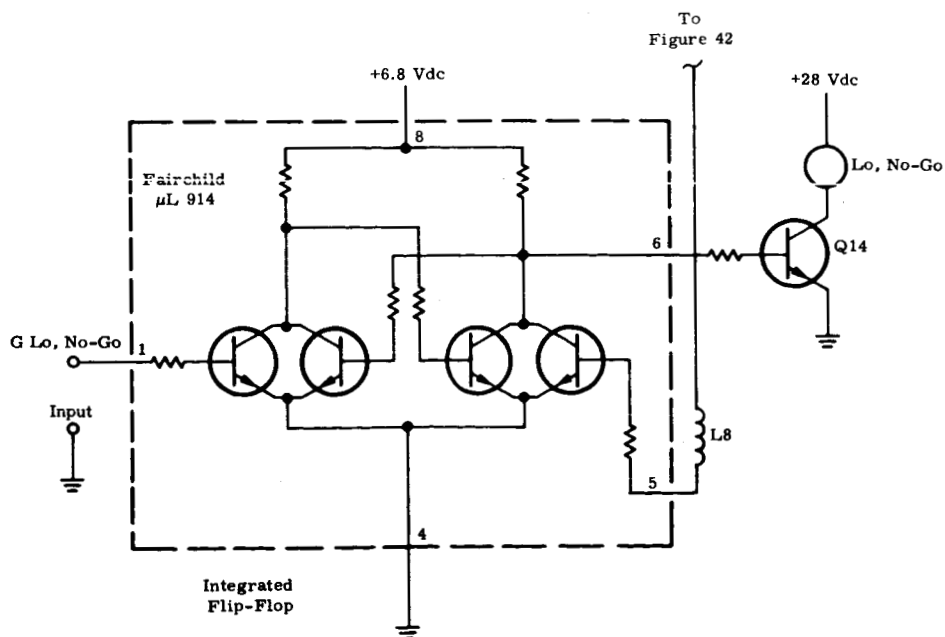


Figure 43. LO, NO-GO Memory and Reset

C. EXTERNAL NOISE

During the development of the visual indicator, it was more practical to use an IR sensor simulator. The simulator was designed to generate essentially the same waveform produced by the IR sensor during an actual weld. Development was progressing as expected until the marriage of the visual indicator to the welding system when erratic operations began. It was discovered that the welder generated spikes of voltages in the visual indicator both preceding and following the IR signal. The sensitivity of the indicator to these spikes was reduced sufficiently by inserting low pass filters to permit a feasibility demonstration.

D. FUTURE CIRCUIT IMPROVEMENTS

Problems experienced with the breadboard visual indicator would be eliminated or greatly improved by the following changes:

- 1 From the voltage generated between the welding electrodes, establish a signal that must be "and" with output signal from any one of the signal level detectors to trigger its memory module. This circuit will greatly reduce the sensitivity of the visual indicator to most externally generated noise.
- 2 Investigate the use of Zenor diodes and associated resistors to eliminate the need for a sensor voltage control.
- 3 Investigate the elimination of coarse and fine zero controls by using the transistor resistance as part of the sensor load resistor. When sensor resistance increases, the resistance of the transistor is made to increase, thereby not allowing zero reference to move.

III. PSEUDOWELD FEASIBILITY

The second phase of this program deals with the use of a pseudoweld (or low energy weld) as an in-process technique for predicting the relative quality of a full energy weld. The equipment setup is shown in Figure 44. For this purpose the IR was measured while a weld energy level insufficient to cause sticking was applied to the various lead-ribbon material combinations. Without disturbing the lead-ribbon material setup, the power level was then increased and a full strength weld performed. Again the IR emission was recorded and the tensile strength of the weld determined. For comparison purposes, a full strength weld was made without the pseudoweld. The measured IR and weld strength for these conditions were also recorded.

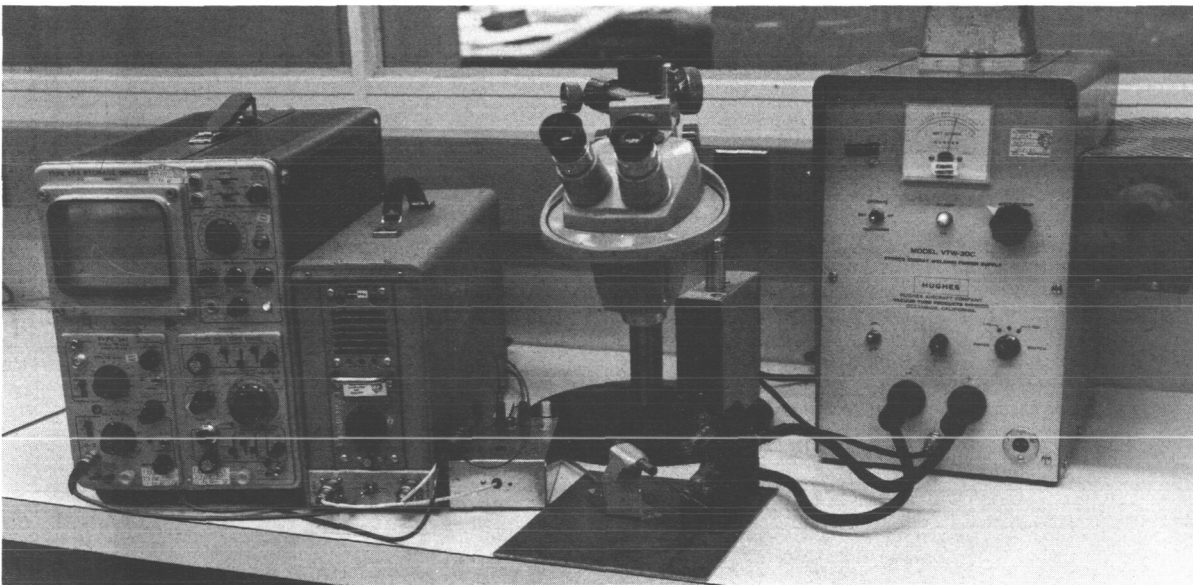


Figure 44. Pseudoweld Equipment

As an extension of the pseudoweld concept, it was postulated that a condition, which could potentially cause a defective weld although unobserved by the operator, could be detected at a low energy level and corrected before committing the joint to a full energy weld. To prove this concept, a series of defective or objectionable weld conditions were simulated in the laboratory. Included in the defective weld conditions were:

- 1 Reversed lead-ribbon polarity
- 2 Oxidized lead materials
- 3 Reduced internal lead-ribbon angle
- 4 Off-center lead-ribbon placement
- 5 Greasy lead material.

Since it is known that the surface conditions (i.e., oxidation) of the lead material directly effects the weld quality it was decided that the leads should be subjected to the same heat cycles experienced during electronic component fabrication. Several manufacturers were contacted; the consensus being that the maximum temperature employed was 575°F. The lead materials were heated at this temperature until any slight discoloration was noted. The time cycle varied from 5 minutes to 1 hour. The welds were performed at normal parameters. Weld strength was not adversely affected when compared to standard conditions therefore this condition was not classified as defective.

Welds were made using other supposed objectionable conditions but it became obvious that if the contaminant was sparsely placed, either an acceptable weld or no weld was achieved depending on location of contaminants. The investigation was therefore limited to the above noted conditions.

The pseudoweld portion of this program was carried out using the three basic lead materials 0.020 inch Dumet, 0.017 inch Kovar, and 0.020 inch Nickel wire with 0.010 by 0.020 inch Nickel as the interconnecting ribbon. Both gold plated and bare leads were welded using bare interconnecting material. Twenty-five pseudowelds followed by a full strength weld were made for each material combination. The pseudoweld energy was set so that no sticking between components was evident. For comparison purposes, a full strength weld without the pseudoweld was made to investigate the effect of the low energy pulse. The IR emission for each weld was measured on a Tektronic Type 564 Storage Oscilloscope. In order to achieve added sensitivity, the pseudoweld IR emission was amplified 70 times. A statistical analysis of the data has been made and is presented as Table VI. The value for pseudoweld IR shown is the amplified reading. In the table, \bar{X} is the mean IR output and S is the standard deviation. The 90/95 limits refer to the confidence-probability limits that have been established based on the spread of the data and the sample size. The percent maximum deviation is expressed as KS/\bar{X} , the positive or negative deviation from the mean.

TABLE VI

Statistical Analysis of Infrared Data from Pseudoweld Program

Material	Parameters	Pseudoweld Only				Pseudo-Full Strength Weld				Full Strength Weld Only				Avg Weld Strength
		\bar{X}^*	S	90/95		\bar{X}	S	90/95		\bar{X}	S	90/95		
				Limits	% Dev† (max)			Limits	% Dev (max)			Limits	% Dev (max)	
0.017 Kovar (gold plated)	10 lb pressure 1.5/3.5 WS	0.176	0.0267	$\frac{0.110}{0.242}$	37.6	0.139	0.0074	$\frac{0.121}{0.158}$	13.2	0.117	0.0100	$\frac{0.092}{0.142}$	21.2	11.1
0.017 Kovar (bare)	10 lb pressure 1.5/3.5 WS	0.284	0.039	$\frac{0.188}{0.380}$	33.8	0.155	0.011	$\frac{0.128}{0.182}$	17.4	0.124	0.0145	$\frac{0.088}{0.160}$	29.0	9.7
0.020 Dumet (gold plated)	8 lb pressure 2.5/7.0 WS	0.190	0.032	$\frac{0.111}{0.269}$	41.6	0.116	0.020	$\frac{0.067}{0.165}$	42.2	0.118	0.0161	$\frac{0.078}{0.158}$	33.7	10.4
0.020 Dumet (bare)	8 lb pressure 2.5/7.0 WS	0.140	0.023	$\frac{0.083}{0.197}$	40.7	0.105	0.0212	$\frac{0.053}{0.158}$	49.9	0.096	0.0185	$\frac{0.051}{0.142}$	47.5	9.6
0.020 Nickel (gold plated)	10 lb pressure 2.5/7.0 WS	0.154	0.013	$\frac{0.122}{0.185}$	20.7	0.062	0.0031	$\frac{0.054}{0.071}$	13.0	0.084	0.009	$\frac{0.061}{0.106}$	26.7	11.0
0.020 Nickel (gold plated)	2 lb pressure 1.0/5.0 WS	0.064	0.0153	$\frac{0.027}{0.102}$	58.8	0.085	0.0074	$\frac{0.067}{0.104}$	21.5	0.104	0.0089	$\frac{0.082}{0.126}$	21.2	11.3
0.025 Nickel (bare)	10 lb pressure 2.5 WS	0.214	0.0282	$\frac{0.150}{0.278}$	30.0									
0.025 Nickel (gold plated)	10 lb pressure 3.0 WS	0.291	0.0290	$\frac{0.225}{0.357}$	22.7									

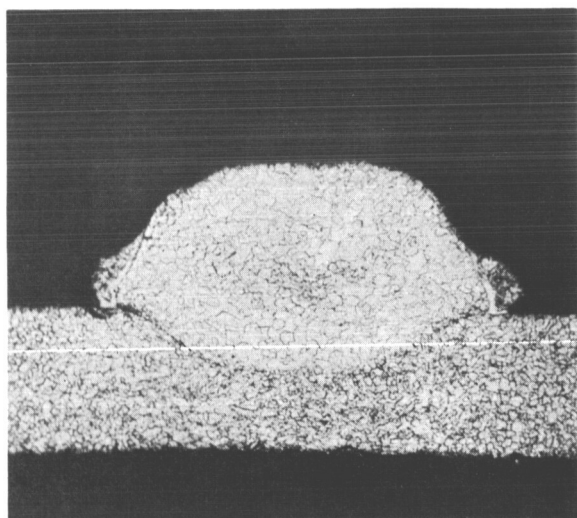
*IR amplified 70 times

†% maximum deviation, $\frac{KS}{\bar{X}}$

In the formulation of the pseudoweld technique, it was postulated that the IR emission could be maintained within limits which were more restrictive than that for a full strength weld since the erratic heat experienced during fusion was not present.

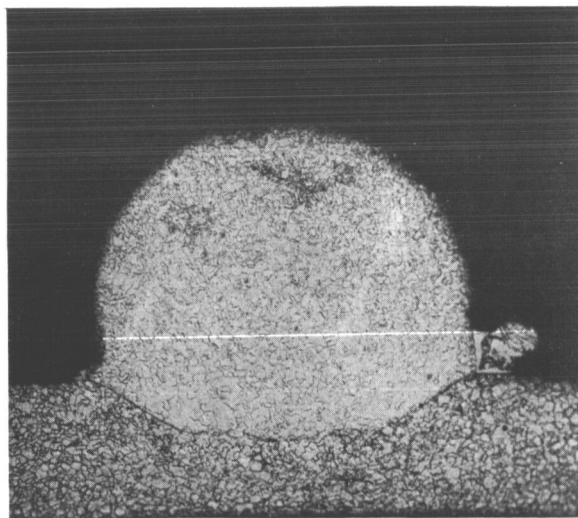
Reviewing the percent maximum deviation data for gold plated Dumet shows that the pseudoweld had little effect on the IR range when associated with a subsequent full strength weld. However, the data for a full strength weld only show a reduced range indicating that the pseudoweld improved IR range control. Conversely, the pseudoweld did not appear to have any effect on the IR range for bare Dumet lead welds.

Selecting the 10 pound pressure level for investigation of gold plated Nickel lead welds, the data in Table VI show that the IR range is reduced by preceding a full strength weld with a pseudoweld when compared with the full strength weld alone. This phenomenon is best explained by the photomicrographs shown in Figure 45. The pseudo-full strength weld for the Nickel lead material does not exhibit the distortion seen in the full strength weld. It is theorized that the pseudoweld allows intimate contact between lead and ribbon thus reducing the interfacial resistance at this joint. In addition the pseudoweld pulse will remove surface oxides and contaminants if present. When the high energy weld is applied to this joint, the reduced resistance results in less heat buildup and therefore less distortion at the weld joint.



(a)

Full Strength Weld Only



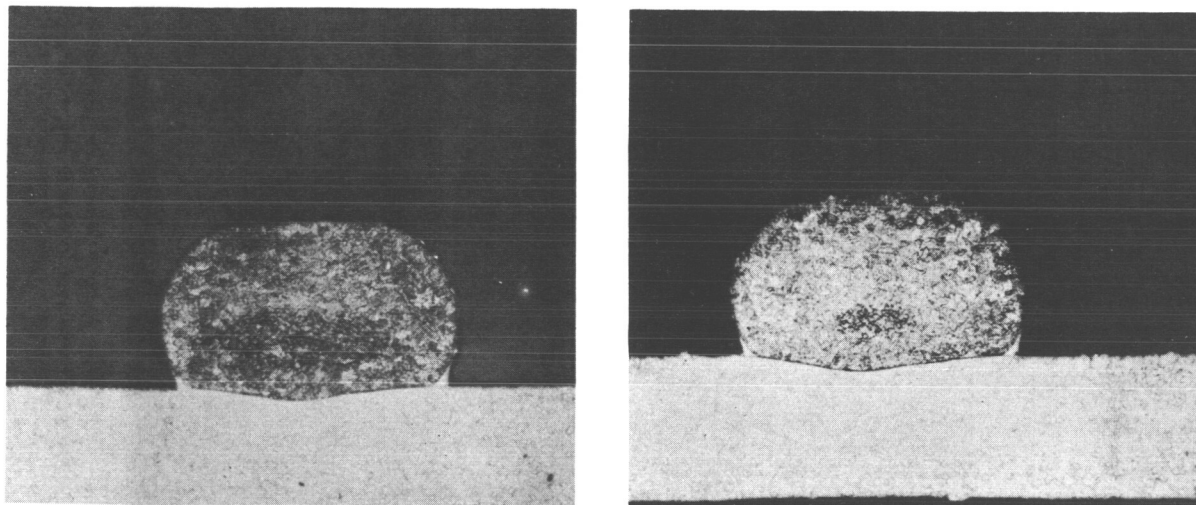
(b)

Pseudo-Full Strength Weld

Figure 45. Effect of Pseudoweld on Weld Quality, Nickel Wire

The 2 pound pressure level for Nickel wire was examined based on the data shown in Table III with the expectation of further reducing the IR data spread. The Nickel lead material is quite pressure dependent as seen in Table VI when considering pseudo and pseudo-full strength weld. A higher pressure is therefore required in order to retain the IR readings within reasonable bounds. This pressure sensitivity is not as evident however when a weld is made without the pseudoweld.

Photomicrographs showing the "pseudo-full strength versus full strength weld" differences are shown in Figure 46 for gold plated Kovar. It can be seen that the weld deformation is not as pronounced as in Figure 45 for Nickel lead material. Slight differences in setdown are attributed to the slight change of interfacial resistance induced by pseudowelding. This would tend to indicate that the pseudo-full strength weld could or should be made with somewhat higher watt-second settings. However, no significant loss of weld strength was noted by use of the pseudoweld when submitted to statistical analysis.



(a)

Full Strength Weld Only

(b)

Pseudo-Full Strength Weld

Figure 46. Effect of Pseudoweld on Weld Quality, Kovar Wire

It is interesting to note that gold plating any of the lead materials has little or no effect on the IR data spread when pseudoweld is considered independently. However, data for the full strength or pseudo-full strength welds show a more restrictive range for the gold plated over bare leads.

If the pseudoweld concept is to be useful as an in-process inspection tool to detect potential defective welds, a discrete IR population must be

observed. A series of conditions that were known to produce either defective welds or typical undesirable production conditions were simulated in the laboratory.

Of all these conditions investigated, only two produced defective welds as basic criteria in judging a welding condition defective. These were weld lead angularity and reverse polarity. The other conditions, while introducing a wider spread in IR data, did not produce defective welds. All tensile data of the other "supposed" defective welds more than exceeded the 60 percent minimum base metal strength.

To simulate contaminate conditions, which may be encountered on the production floor, several grease base materials were evaluated to produce controlled defects. These contaminants, as mentioned previously, were oil, cosmoline, lipstick, and facial grease. These contaminants produced sound welds of high strength. The contaminants appeared to volatilize during welding without leaving any trace in the immediate vicinity of the weld nugget. During the welding cycle, contact of the welding leads is made through the contaminate by the applied weld pressure. The localized resistive heating appears to volatilize the contaminant, blowing bulk contaminants and the gaseous air environment away from the molten nugget. In fact, several welds made in this manner were very clean and bright. Since defective welds were not produced, this form of contaminate was not investigated further. This effect will be reexamined at a later date for potential beneficial effects.

For this study, two populations were run, one under ideal standard conditions, and the other under controlled conditions planned to produce defective welds. This data was statistically analyzed to establish data spread according to a 90 percent confidence level and a 95 percent probability.

A table was compiled of the two conditions which produced defective welds, the percentage of defective welds produced, and the population separation demonstrated by the pseudoweld concept (Table VII).

For the first defective condition, angularity, significant separation of the standard and defective population was achieved in the pseudoweld IR pulse data. While some sound welds were present in defective populations for Kovar and Nickel, the weight of the defective data was sufficient to produce 100 percent separation of the pseudoweld IR pulse data. In the case of Dumet, 60 percent defective welds produced a minus 74 percent separation of pseudoweld IR pulse data.

In the second defective condition, weld current polarity was reversed. Some metal-metal or metal-oxide systems are known to resist, or in some

TABLE VII

Detection of Undesirable Welds

Material (Gold Plated)	Angularity			Reverse Polarity	
	Test Angle (deg)	Pop Separation (%)	% Defect	Pop Separation (%)	% Defect
Kovar	35	100	92	+40	None
Dumet	45	-74	60	-40	52
Nickel	35	100	52	0	None

cases assist, the flow of current when polarity is reversed due to self rectification or the thermocouple effect. Only in Dumet did this phenomenon appear to produce significant detrimental effects. In both populations of Kovar and Nickel, no detrimental effects were observed, weld strength was not effected. In the case of Kovar, the population welded with reverse polarity registered higher IR values than that welded with straight polarity. IR data for the Nickel populations showed no significant difference. In the case of Dumet, a 52 percent defective population was registered in tensile testing on the population welded with reverse polarity. IR data showed an effective lowering of the heat input sufficient to produce a population separation of -40 percent.

Since population limits are derived by statistical analysis, these limits are largely dependent upon population size. In this study a population of 25 was used to derive these results. A larger population would produce more closely correlatable data. For instance, population separation of Dumet data when welded under reverse current conditions would more closely match the percent defective welds observed.

Population separations on the lower side of the standard condition correlates with the production of defective welds. Population separation on the positive side does not correlate with defective welds because a little more heat than that chosen for the standard condition still produces sound welds

Thus, we have found that the pseudo weld concept has exhibited the capability to predict weld quality by the detection of undesirable preweld conditions. With this capability, decision to-weld or not-to-weld may ultimately be made by man or machine logic.

PRECEDING PAGE BLANK NOT FILMED.

RECOMMENDATIONS

As a direct outgrowth of the work performed on the present contract, Study on Development of Techniques for Resistance Welding Systems," the following recommendations and their descriptions represent a further development program in logical steps for the welding system for higher density packaging, as conceived by the Orlando division of Martin Marietta Corporation.

- 1 Develop an in-process, nondestructive test-and-control apparatus utilizing infrared techniques compatible with high volume production requirements.
 - a This would include design features that overcome such problems as electrical noise generated by surrounding equipment, line voltage variations, long term stability without daily calibration, simplicity in set-up and operation procedures, and simple calibration procedures.
 - b A new feature to be added is the lockout control of the weld pulse supply. In the advent of an unacceptable weld, the lockout circuit will render the power supply inoperable and a visual NO-GO indication will be given.
- 2 Develop the in-process, pre-weld Martin inspection technique utilizing the pseudoweld concept.
 - a It is recommended that additional work be performed to establish more valid limits to permit the use and incorporation of the pseudoweld concept into an advanced welding system which may be added to existing production equipment on the production line or into a completely new welding package power supply.
 - b The basic concept lends itself to automatic lockout whereby a full strength weld cannot be made unless optimum welding conditions are predicted by the initial pseudoweld.

- c System requirements will be established for the pseudowelding equipment based upon the extensive data resulting from the present contract which includes many thousands of statistical experiments. This equipment will be capable of automatically analyzing the emitted IR during pseudoweld pulses and will provide a visual GO or NO-GO indication. If the indication is NO-GO, a fusion weld will be prevented. If the indication is GO, a fusion weld pulse is allowed.
- 3 Determine the feasibility of developing a completely new type of power supply to incorporate an optimum heat pulse shape through the use of IR feedback control.
 - a Many variables are associated with the resistance welding process. One of the most troublesome of those variables, made evident from our studies, is weld pulse magnitude variation from weld to weld for any fixed watt-second setting of the welding power supply. Poor welds are often the result. This problem could be eliminated if the IR heat generated at the weld joint is sensed and automatically increased or decreased by closed-loop feedback control to the weld power supply during the weld pulse.
 - b The correlation between IR energy emitted from the weld during the welding process and weld quality was conclusively established on the present contract. Since the strength of the weld joint is directly related to the IR output, it is ideally suited as a feedback control for the weld power supply. By using the IR output as a feedback control, compensation would be made automatically for the many variations in the welding process and in component lead materials. Each weld would then result in a good weld and many of the problems would be eliminated.

REFERENCES

1. Mills, G. W., "A Comparison of Permanent Electrical Connections," The Bell System Technical Journal, Vol XLIII No. 3, May 1964
2. Martin Marietta Corporation Internal Report, "Contactless Continuity Measurements," G. D. Yates, December 1965
3. Sears, F. W., "Optics," Third Edition, p 316, 1958